

Neural Network Machine Regression (NNMR): A Deep Learning Framework for Uncovering High-order Synergistic Effects

Jiuchen Zhang

Department of Biostatistics, University of Michigan

and

Ling Zhou

Center of Statistical Research and School of Statistics,

Southwestern University of Finance and Economics

and

Peter Song

Department of Biostatistics, University of Michigan

February 3, 2026

Abstract

We propose a new neural network framework, termed Neural Network Machine Regression (NNMR), which integrates trainable input gating and adaptive depth regularization to jointly perform feature selection and function estimation in an end-to-end manner. By penalizing both gating parameters and redundant layers, NNMR yields sparse and interpretable architectures while capturing complex nonlinear relationships driven by high-order synergistic effects. We further develop a post-selection inference procedure based on split-sample, permutation-based hypothesis testing, enabling valid inference without restrictive parametric assumptions. Compared with existing methods, including Bayesian kernel machine regression and widely used post hoc attribution techniques, NNMR scales efficiently to high-dimensional feature spaces while rigorously controlling type I error. Simulation studies demonstrate its superior selection accuracy and inference reliability. Finally, an empirical application reveals sparse, biologically meaningful food group predictors associated with somatic growth among adolescents living in Mexico City.

Keywords: post-selection inference, depth regularization, input gating

1 Introduction

In many scientific fields, such as biomedical research, genomics, epidemiology, and environmental science, researchers work with high-dimensional datasets where the number of potential explanatory variables far exceeds the number of observations. Identifying a relevant subset of variables is crucial for improving model interpretability, reducing overfitting, and enhancing predictive performance.

Variable selection has a long history in linear modeling, where sparsity penalties such as the LASSO ([Tibshirani 1996](#)) and smoothly clipped absolute deviation (SCAD; [Fan & Li 2001](#)) are now routine. However, many scientific questions involve nonlinear, possibly high-order interactions that lie well beyond the scope of linear assumptions. To accommodate such complexity, research has shifted toward nonparametric frameworks that let the data reveal flexible functional forms while still isolating the influential predictors. Early efforts extended the linear model to additive structures in which each covariate enters through an unspecified univariate function ([Hastie 2017](#)). Although additive models inherit interpretability and can be equipped with component-wise selection rules, they may miss interaction effects unless higher-order additive terms or interaction kernels are incorporated, a step that greatly complicates both estimation and feature selection.

Complementary strategies tackle the “curse of dimensionality” by screening rather than penalizing. Sure independence screening (SIS; [Fan & Lv 2008](#)) and its variants rank predictors through marginal utilities to select the feature space before more elaborate modeling; however, their reliance on marginal signals can overlook variables that act solely through interactions. Fully Bayesian machinery, typified by Bayesian kernel machine regression (BKMR; [Bobb et al. 2015](#)), integrates variable selection, nonlinear response surfaces, and uncertainty quantification in a single coherent framework, but at the expense of Markov chain Monte Carlo computation that scales poorly with thousands of samples or

covariates. Collectively, these developments underscore a persistent tension in nonparametric regression: balancing modeling flexibility, statistical efficiency, computational feasibility, and interpretability.

Deep neural networks pose a dual challenge for feature selection: the parameterization is massively over-complete, yet the correspondence between weights and inputs is highly entangled. Post hoc attribution tools such as SHAP (Lundberg & Lee 2017), Integrated Gradients (Sundararajan et al. 2017), and deepLIFT (Shrikumar et al. 2017) estimate ex post importance scores by propagating gradients or relevance values back to the input layer. These methods require only a trained model and are widely used in practice, but they do not impose sparsity during training; their scores can be unstable under collinearity and provide no formal guarantee that low-scoring variables are irrelevant—limitations that become acute in high-dimensional biomedical applications.

To induce sparsity within neural networks, two embedded approaches have been proposed. Deep feature selection inserts a sparse linear layer at the network input and applies an ℓ_1 penalty to its weights, thereby jointly learning both a representation and feature importance in an end-to-end fashion (Li et al. 2016). Building on this framework, nonlinear variable selection methods introduce a continuous ℓ_0 relaxation to selection layer, yielding rigorous convergence guarantees and selection consistency under a generalized stable Hessian condition (Chen et al. 2021). Group Lasso regularization instead treats all outgoing connections of each input variable as a group, which prunes entire neurons or inputs to produce highly compact networks without extensive manual grouping (Scardapane et al. 2017). However, these methods still lack automated control over both network depth and width, offer limited support for valid post-selection inference.

In this paper, we propose a neural network-based variable selection method tailored to effectively identify relevant features in high-dimensional settings. Our approach incorporates

several innovations that enhance interpretability, scalability, and statistical rigor. First, we introduce a trainable feature-gating mechanism at the neural network’s input layer, where each feature is weighted by a learnable parameter. Coupled with an L_1 -penalty analogous to the LASSO (Tibshirani 1996), this mechanism directly induces sparsity, explicitly identifying a concise subset of predictors most strongly associated with the outcome.

Second, our method includes an adaptive thresholding procedure during training, periodically removing features whose gating parameters remain persistently small. Additionally, we dynamically prune redundant hidden layers by replacing them with identity mappings if their contributions become negligible. These two procedures promote structured sparsity across both input features and network depth, resulting in a compact and interpretable model.

Third, we establish theoretical guarantees for our approach by deriving an risk upper bound, achieving minimax optimality under mild conditions. Combined with our proposed data-splitting and permutation-based inference framework, our method rigorously controls type-I errors in high-dimensional analyses, effectively reducing false discoveries.

Our neural network-based variable selection approach exhibits several advantages over existing methods, particularly in contexts involving large-scale biomedical and genetic data. Unlike Bayesian kernel machine regression (BKMR) (Bobb et al. 2015), which involves computationally expensive kernel inversions, or traditional screening approaches (Fan & Lv 2008), our framework scales efficiently to hundreds or even thousands of predictors. Moreover, in contrast to popular post hoc interpretation methods such as SHapley Additive exPlanations (SHAP) or Integrated Gradients—often unstable or misleading in high-dimensional settings—our method directly incorporates interpretability within the model training process through structured penalties.

Overall, our unified framework simultaneously addresses feature selection, adaptive neural

network optimization, and rigorous statistical inference, positioning our method as a powerful advancement for interpretable, scalable, and statistically rigorous feature selection in contemporary statistical modeling and deep learning applications.

2 Methodology

We consider variable selection within the framework of neural networks. Suppose we observe independent and identically distributed samples $\{(\mathbf{X}_i, Y_i)\}_{i=1}^n$, where $Y_i \in \mathbb{R}$ is a scalar response and $\mathbf{X}_i \in \mathbb{R}^d$ is a high-dimensional vector of predictors. Our objective is to simultaneously estimate the unknown relationship $g(\cdot)$ between predictors and response, and identify a sparse subset of relevant features. To accomplish this, we embed the variable selection directly into the neural network training process. Specifically, we estimate g by minimizing the empirical squared-error loss:

$$\hat{g} = \arg \min_{g \in \mathcal{G}} \frac{1}{n} \sum_{i=1}^n (Y_i - g(\mathbf{X}_i))^2, \quad (1)$$

where \mathcal{G} denotes the class of neural networks designed explicitly to perform variable selection.

2.1 Neural Network

We set \mathcal{G} to be a function class consisting of multi-layers neural networks with a ReLU activation function to approximate the conditional expectation:

$$\mathcal{G} := \mathcal{NN}(\mathcal{W}, \mathcal{D}, \mathcal{S}, \mathcal{B}),$$

where the input data is the predictor \mathbf{X}_i , forming the first layer, and the output is the last layer of the network. This network \mathcal{G} has width \mathcal{D} , which includes \mathcal{D} hidden layers and $\mathcal{D} + 2$ total layers. Let N_l denote the width of layer l for $l = 0, \dots, \mathcal{D}, \mathcal{D} + 1$, which is the number of nodes in each layer. Specifically, $N_0 = d$ represents the input dimension of X ,

and $N_{\mathcal{D}+1} = 1$ represents the response Y . The width \mathcal{W} is the maximum width among the hidden layers:

$$\mathcal{W} = \max(N_1, \dots, N_{\mathcal{D}}).$$

Without loss of generality, we consider the same width for all hidden layers in this paper. The size \mathcal{S} is the total number of parameters in the network \mathcal{G} , given by $\mathcal{S} = \sum_{l=0}^{\mathcal{D}} N_{l+1} \times (N_l + 1)$.

In particular, a ReLU neural network with \mathcal{D} hidden layers is a collection of mappings $g : \mathbb{R}^{N_0} \rightarrow \mathbb{R}^{N_{\mathcal{D}+1}}$ of the form $g(\mathbf{x}) = h_{\mathcal{D}} \circ \sigma \circ h_{\mathcal{D}-1} \circ \dots \circ \sigma \circ h_0(\mathbf{x})$, where $h_1 \circ h_2(\mathbf{x}) := h_1(h_2(\mathbf{x}))$ represents the composition of two functions h_1 and h_2 ; $\sigma(\mathbf{x}) := \max(\mathbf{x}, 0)$ is the ReLU function, which is applied elementwise; $h_l(\mathbf{x}) := \mathbf{W}_l \mathbf{x} + c_l$ is an affine transformation with $\mathbf{W}_l \in \mathbb{R}^{N_{l+1} \times N_l}$ and $c_l \in \mathbb{R}^{N_l}$. We assume that every function $g \in \mathcal{G}$ satisfies $\|g\|_{\infty} \leq \mathcal{B}$ for some $0 < \mathcal{B} < \infty$, where $\|g\|_{\infty}$ is the supnorm of the function g .

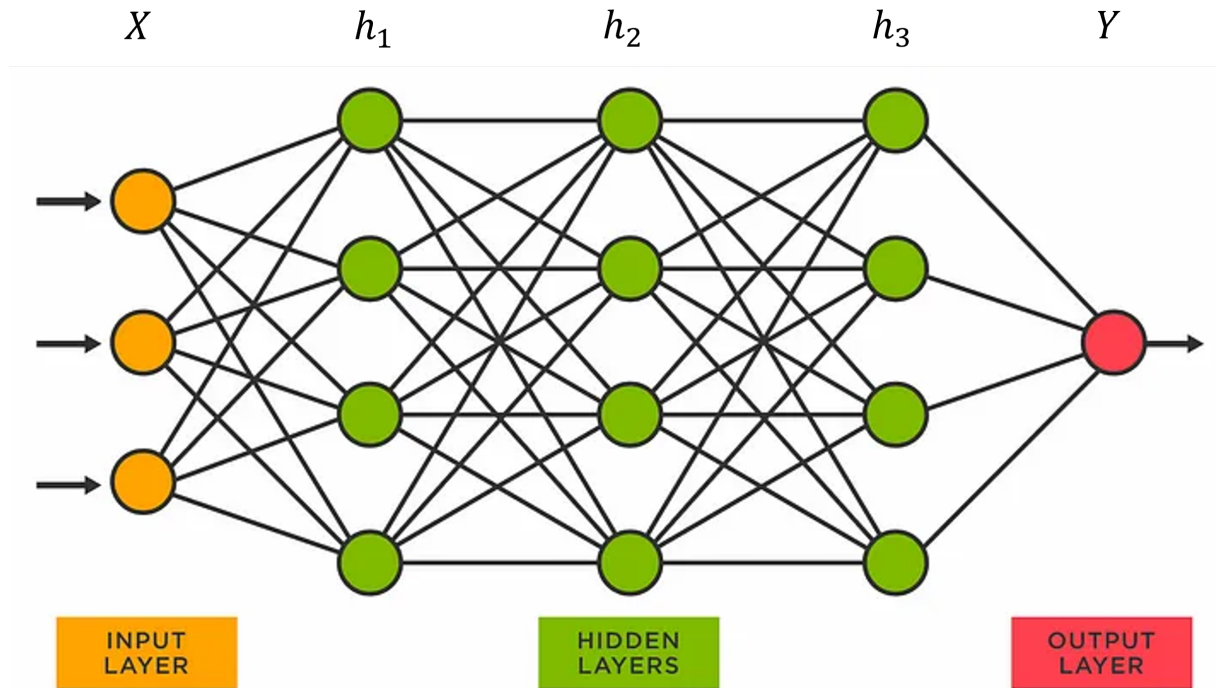


Figure 1: Simple Multi-layer Neural Network

2.2 Variable Selection

In high-dimensional nonparametric regression problems, the response variable Y often depends on only a small subset of the available features, while the rest contribute little to predictive accuracy. This suggests that the data lies on a low-dimensional manifold embedded in the high-dimensional feature space. By leveraging this assumption, we aim to identify and retain only the most relevant features, reducing computational complexity while maintaining predictive performance.

To exploit this sparsity we attach to the input layer a trainable gating vector $\boldsymbol{\alpha} = (\alpha_1, \dots, \alpha_d)^\top \in \mathbf{R}^d$ and feed the re-weighted input

$$\widetilde{\mathbf{X}} = \boldsymbol{\alpha} \odot \mathbf{X}, \quad (\boldsymbol{\alpha} \odot \mathbf{X})_j = \alpha_j X_j,$$

into the network.

This transformation allows the model to learn which features are important by setting some entries of α to zero, effectively removing those variables from consideration. The resulting feature selection mechanism is embedded within the neural network architecture, ensuring that only a subset of the input dimensions contributes to the final model.

To formalize the selection process, we incorporate L_1 regularization on α , which encourages sparsity by penalizing small coefficient values. If α has exactly d_0 nonzero elements, then $\widetilde{\mathbf{X}}$ can be viewed as a d_0 -dimensional vector, allowing the model to learn a function $g : \mathbb{R}^{d_0} \rightarrow \mathbb{R}$. This leads to the following optimization problem:

$$\mathcal{L}_n(g) = \frac{1}{n} \sum_{i=1}^n \left\{ Y_i - g(\mathbf{X}_i) \right\}^2 + \lambda_1 \|\boldsymbol{\alpha}\|_1,$$

Here, $g \in \mathcal{G}(\boldsymbol{\alpha}, \boldsymbol{\theta})$ is a neural network that maps the selected features to Y , where $\mathcal{G}(\boldsymbol{\alpha}, \boldsymbol{\theta}) = \{g : g = \phi(\boldsymbol{\alpha} \odot \mathbf{X}), \phi \in \mathcal{G}\}$, $\boldsymbol{\theta} = (\mathbf{W}_l, c_l, l = 0, \dots, \mathcal{D})$, and $\|\cdot\|_1$ serves as an L_1 norm that ensures sparsity in $\boldsymbol{\alpha}$. This formulation not only selects the most informative features

but also learns the nonlinear mapping between those features and the response variable. Unlike traditional feature selection methods that operate in a separate preprocessing step, our approach integrates feature selection into the model training process, allowing it to dynamically adapt the selected features based on the data.

Compared to existing feature selection techniques such as Bayesian Kernel Machine Regression (BKMR) and SHAP-based methods, our approach offers significant advantages in terms of scalability and efficiency. BKMR, while powerful in modeling nonlinear interactions, suffers from high computational costs due to kernel matrix inversion, making it impractical for large-scale problems. Similarly, SHAP-based methods, which estimate feature importance post hoc, do not enforce sparsity and can be computationally expensive for high-dimensional data.

In contrast, our method is fully compatible with GPU-accelerated deep learning frameworks, allowing it to scale efficiently. The integrated feature selection mechanism eliminates the need for separate preprocessing steps, reducing overhead. Moreover, by explicitly learning a sparse representation, our approach ensures that the model remains interpretable while retaining predictive power.

The input-gating layer reduces the width of the effective feature space, but the depth of the network remains fixed. Retraining a new architecture each time the size of the active set changes is computationally infeasible. Following [Tan et al. \(2024\)](#), a hidden layer l is redundant when its linear map $h_l(x) = \mathbf{W}_l x$ simply forwards its input, i.e. $\mathbf{W}_l = \mathbf{I}$ and $c_l = 0$, where \mathbf{I} is the identity matrix. Note that the bias term has been absorbed into the augmented input.

This motivates the depth penalty,

$$\text{DP}(\theta) = \sum_{l=1}^{\mathcal{D}} (\|\mathbf{W}_l - \mathbf{I}\|_1 + |c_l|),$$

which is zero precisely when every dispensable layer collapses to the identity. Combining input gating and depth regularisation, the final training problem becomes

$$(\hat{\boldsymbol{\alpha}}, \hat{\boldsymbol{\theta}}) = \arg \min_{g \in \mathcal{G}(\boldsymbol{\alpha}, \boldsymbol{\theta})} \left\{ \frac{1}{n} \sum_{i=1}^n \left\{ Y_i - g(\mathbf{X}_i) \right\}^2 + \lambda_1 \|\boldsymbol{\alpha}\|_1 + \lambda_2 \sum_{l=1}^{\mathcal{D}} (\|\mathbf{W}_l - \mathbf{I}\|_1 + |c_l|) \right\}, \quad (12)$$

with λ_1 controlling sparsity and λ_2 regulating depth. During optimization each \mathbf{W}_l is softly shrunk toward the identity matrix whose penalty terms converge to zero can be pruned after training, yielding a compact architecture that matches the complexity of the selected feature subset while retaining the expressive power of deep ReLU networks.

2.3 Inference Procedure after Variable Selection

Following variable selection, rigorous statistical inference is required to assess the significance of the retained predictors. We employ a data-splitting strategy (Cox 1975, Hurvich & Tsai 1990) combined with the model-free test of conditional independence (Cai et al. 2022). Specifically, we partition the sample into two parts—one for both variable selection and estimation of conditional mean functions, and the other solely for inference—thereby preserving maximum power.

Specifically, we divide the original dataset into two subsets: one for variable selection and estimation (denoted D_1), and another purely for inference (denoted D_2). The first subset D_1 is used both to identify important predictors through the penalized neural network described in Section 2.2 and to estimate conditional expectations for inference purposes. The inference step directly utilizes the entire second subset D_2 without further splitting, enhancing statistical power.

Let the selected variables identified from D_1 be represented as \mathbf{X}_S . The inference procedure involves testing the null hypothesis:

$$H_0 : E(Y | \mathbf{X}_{-j,S}) = E(Y | \mathbf{X}_S) \quad \text{versus} \quad H_1 : E(Y | \mathbf{X}_{-j,S}) \neq E(Y | \mathbf{X}_S),$$

where \mathbf{X}_j denotes potential variable of interest and $\mathbf{X}_{-j,S}$ denotes the rest of variables in \mathbf{X}_S excluding \mathbf{X}_j .

Following the methodology of [Cai et al. \(2022\)](#) with our enhanced approach, we fit two nonparametric models using data from D_1 : one model incorporating both X_S and Z , denoted by $\hat{g}_1(\mathbf{X}_S)$, and a null model that includes only $\mathbf{X}_{-j,S}$, denoted by $\hat{g}_0(\mathbf{X}_{-j,S})$. To assess the predictive performance of these models, we perform two-sample comparisons on the residuals from these models using the inference dataset D_2 . Specifically, we utilize the two-sample t-test (TS), defined as the average difference in squared residuals between the two models. The test statistic T_{TS} is computed as:

$$T_{TS} = \frac{1}{n_2} \sum_{i \in D_2} \left[\{Y_i - \hat{g}_1(\mathbf{X}_{S,i})\}^2 - \{Y_i - \hat{g}_0(\mathbf{X}_{-j,S,i})\}^2 \right],$$

and we reject the null hypothesis H_0 if T_{TS} is significantly negative. This test evaluates the difference in mean squared prediction errors between the two models, under the assumption that second-order moments exist for the data.

Algorithm 1: Inference procedure with permutation testing

Input: Training data D_1 , inference data D_2 , number of permutations B , selected

variable \mathbf{X}_S obtained from D_1

Output: Test statistic and p-value

- 1 Estimate $\hat{g}_1(\mathbf{X}_S)$ and $\hat{g}_0(\mathbf{X}_{-j,S})$ using D_1 ;
- 2 Evaluate both models on D_2 and calculate residuals:
- 3 $U_i = Y_i - \hat{g}_1(\mathbf{X}_{S,i})$,
- 4 $V_i = Y_i - \hat{g}_0(\mathbf{X}_{-j,S,i})$, for all $i \in D_2$;
- 5 Define the pooled set $S = \{U_i\} \cup \{V_i\}$;
- 6 Compute observed test statistic T using $\{U_i\}, \{V_i\}$;
- 7 **for** $b = 1$ to B **do**
 - 8 Randomly partition S into two equal-sized sets $\{U_i^*\}, \{V_i^*\}$;
 - 9 Compute test statistic $T_{TS,b}^*$ using $\{U_i^*\}, \{V_i^*\}$;
- 10 Compute p-value: $\hat{p}_{TS} = \frac{1}{B} \sum_{b=1}^B I\{T > T_{TS,b}^*\}$;

The significance of this incremental predictive power is evaluated by permutation tests, as described in Algorithm 1. Estimation of $\hat{g}_1(\mathbf{X}_S)$ and $\hat{g}_0(\mathbf{X}_{-j,S})$ using D_1 increases statistical efficiency and power by fully utilizing the inference dataset, ensuring robust inference without restrictive parametric assumptions. Additionally, our inference framework is flexible, allowing for individual testing of each selected variable separately, or focusing solely on specific variables of particular interest based on the research objectives.

In addition, under suitable conditions, one can show that the asymptotic Gaussianity of the t statistic T_{TS} has been established in [Lei \(2020\)](#). As a result, the last step of the p value calculation can be modified by first estimating the standard derivation of $\{T_{TS,b}^*, b = 1, \dots, B\}$, denoted as $\hat{\sigma}_B$, and then calculating the p value as $\Phi^{-1}(T/\hat{\sigma}_B)$, where Φ is the cumulative distribution function of standard normal distribution. This will provide a p value with

relatively high resolution.

3 Theory

In this section, we present theoretical results concerning the consistency and validity of our neural network-based variable selection approach. We begin by formally defining the theoretical framework underlying our methodology.

Let $X_{[j]}$ be the j -th component of \mathbf{X} . Then $X_{[j]}$ is defined as conditionally unimportant if and only if

$$\mathbb{E}(Y \mid \mathbf{X}_{[-j]} = \mathbf{x}_{[-j]}) = \mathbb{E}(Y \mid \mathbf{X} = \mathbf{x}), \quad (2)$$

where $\mathbf{X}_{[-j]} = (X_{[1]}, \dots, X_{[j-1]}, X_{[j+1]}, \dots, X_{[d]})$, and \mathbf{x}_{-j} is defined similarly.

We assume \mathbf{X} is supported on a bounded set, and for simplicity, we assume this bounded set to be $[0, 1]^d$. In the rest of the paper, the constant c denotes a positive constant that may vary across different contexts. We separate \mathbf{X} into $\mathbf{X}^s \in [0, 1]^{d_0}$ and $\mathbf{X}^c \in [0, 1]^{d-d_0}$, denoting the conditional important and unimportant variables, respectively. For any $\mathbf{x} \in [0, 1]^p$,

$$\mathbb{E}(Y \mid \mathbf{X}^s = \mathbf{x}^s) = \mathbb{E}(Y \mid \mathbf{X} = \mathbf{x}).$$

Let g^* be the minimizer of the population loss, that is,

$$g^* = \arg \min_{g \in \mathcal{H}^\beta([0,1]^p, \mathcal{B})} \mathbb{E} (Y_i - g(\mathbf{X}_i))^2,$$

where the minimizer is taken over the entire space and thus implies that g^* does not necessarily belong to the FNN set $\mathcal{G}(\boldsymbol{\alpha}, \boldsymbol{\theta})$. Clearly, based on the definition (2) $g^*(\mathbf{X})$ depends on \mathbf{X}^s only. To simplify notation, we assume the first d components of \mathbf{X} are important, and divide $\boldsymbol{\alpha}$ into two parts $\boldsymbol{\alpha} = (\boldsymbol{\alpha}_s, \boldsymbol{\alpha}_c)$ with $\boldsymbol{\alpha}_s \in \mathbb{R}^d$ and $\boldsymbol{\alpha}_c \in \mathbb{R}^{p-d}$ corresponding to the coefficients of \mathbf{X}^s and \mathbf{X}^c , respectively.

We establish the large sample property of \hat{g} in terms of its excess risk, which is defined as the difference between the risk of g and g^* :

$$\mathcal{R}(g) - \mathcal{R}(g^*) = \mathbb{E} (Y_i - g(\mathbf{X}_i))^2 - \mathbb{E} (Y_i - g^*(\mathbf{X}_i))^2.$$

We construct an estimator of g^* within $\mathcal{G}(\boldsymbol{\alpha}, \boldsymbol{\theta})$ with network parameters $\boldsymbol{\theta}$ and variable importance index parameters $\boldsymbol{\alpha}$. Thus, referring to the optimal network solution

$$g_{\mathcal{G}}^* = \arg \min_{g \in \mathcal{G}(\boldsymbol{\alpha}, \boldsymbol{\theta})} \mathbb{E} (Y_i - g(\mathbf{X}_i))^2,$$

we define a set of $(\boldsymbol{\alpha}, \boldsymbol{\theta})$ as

$$\boldsymbol{\Theta} = \{(\boldsymbol{\alpha}, \boldsymbol{\theta}) : \mathcal{R}(g_{\boldsymbol{\alpha}, \boldsymbol{\theta}}) = \mathcal{R}(g_{\mathcal{G}}^*), g_{\boldsymbol{\alpha}, \boldsymbol{\theta}} \in \mathcal{G}(\boldsymbol{\alpha}, \boldsymbol{\theta})\}.$$

With proper conditions on the data structure and network class, $g_{\mathcal{G}}^*$ can approach g^* close enough such that $\boldsymbol{\alpha}_c = 0$ and $\boldsymbol{\alpha}_s \neq 0$. That is, for any $(\boldsymbol{\alpha}, \boldsymbol{\theta}) \in \boldsymbol{\Theta}$, there exists a positive constant $c > 0$ such that $\min_{1 \leq j \leq d} |\alpha_j| \geq c$. Further, there exists a solution $\boldsymbol{\alpha}_s \neq 0$, $\boldsymbol{\alpha}_c = 0$ such that $(\boldsymbol{\alpha}_s, \mathbf{0}, \boldsymbol{\theta}) \in \boldsymbol{\Theta}$ still holds. These properties of $g_{\mathcal{G}}^*$ and $\boldsymbol{\Theta}$ are given in Lemma 7.1 in the Supplementary Materials.

In practice, the network parameters $(\hat{\boldsymbol{\alpha}}, \hat{\boldsymbol{\theta}})$ obtained in (12) lies outside of $\boldsymbol{\Theta}$. To measure the distance between $(\boldsymbol{\alpha}, \boldsymbol{\theta})$ and $\boldsymbol{\Theta}$, we define metric $d((\boldsymbol{\alpha}, \boldsymbol{\theta}), \boldsymbol{\Theta}) := \min_{\boldsymbol{\theta} \in \boldsymbol{\Theta}} \|\begin{pmatrix} \boldsymbol{\alpha} \\ \boldsymbol{\theta} \end{pmatrix}\|_2^2$. Clearly, $d((\hat{\boldsymbol{\alpha}}, \hat{\boldsymbol{\theta}}), \boldsymbol{\Theta}) \rightarrow 0$ is sufficient for $\hat{\boldsymbol{\alpha}}_s$ to be bounded away from zero. Thus, we can establish the selection results via establishing the convergence rate of the proposed penalized network $\hat{g}_{\mathcal{G}}$ in terms of its parameters.

We define $\mathcal{G}|_{\mathbf{x}} := \{g(\mathbf{x}_1), g(\mathbf{x}_2), \dots, g(\mathbf{x}_n) : g \in \mathcal{G}(\boldsymbol{\alpha}, \boldsymbol{\theta})\}$ for a given sequence $\mathbf{x} = (\mathbf{x}_1, \dots, \mathbf{x}_n)$ and denote $\mathcal{N}_{2n} = \sup_{\mathbf{x}} \mathcal{N}_{2n}(\delta, \|\cdot\|_{\infty}, \mathcal{G}|_{\mathbf{x}})$ as the covering number of $\mathcal{G}|_{\mathbf{x}}$ under the norm $\|\cdot\|_{\infty}$ with radius δ . Let $A \preceq B$ represent $A \leq cB$ for a positive constant c , $A \wedge B = \min(A, B)$, and $\Phi_1 \circ \Phi_2 := \{\phi_1 \circ \phi_2 : \phi_1 \in \Phi_1, \phi_2 \in \Phi_2\}$ represents the composition of two function classes Φ_1 and Φ_2 .

The next conditions are needed to establish the theoretical results:

(C1) The dimension of conditional important variables d is fixed, and there exists a constant

$\tau_d > 0$ such that

$$\min_{1 \leq j \leq d} \left| \mathbb{E}(Y \mid \mathbf{X}_{[-j]} = \mathbf{x}_{[-j]}) - \mathbb{E}(Y \mid \mathbf{X} = \mathbf{x}) \right| \geq c\tau_d,$$

for some positive constant c .

(C2) Assume Y is a sub-Gaussian random variable.

(C3) Function class for $g_{\alpha, \theta}$ and g^* : for any function $g_{\alpha, \theta} \in \mathcal{G}$ and the true function g^* , we assume $\|g_{\alpha, \theta}\|_{\infty} < \mathcal{B}$ and $\|g^*\|_{\infty} < \mathcal{B}$.

Theorem 3.1 Suppose the conditions (C1)-(C3) hold. If $\lambda_1^2 \preceq \frac{\log^2 n \log \mathcal{N}_{2n}}{nd} + \frac{(\mathcal{R}(g_{\mathcal{G}}^*) - \mathcal{R}(g^*))}{d}$ and $\lambda_2^2 \preceq \frac{\log^2 n \log \mathcal{N}_{2n}}{n \mathcal{W}^2 \mathcal{D}} + \frac{(\mathcal{R}(g_{\alpha, \theta}) - \mathcal{R}(g^*))}{\mathcal{W}^2 \mathcal{D}}$, $(\hat{\alpha}, \hat{\theta})$ defined in (12) satisfies

$$\begin{aligned} \mathbb{E}[d((\hat{\alpha}, \hat{\theta}), \Theta)] &\preceq \frac{\log^2 n \log \mathcal{N}_{2n}}{n} + \log^2 n (\mathcal{R}(g_{\mathcal{G}}^*) - \mathcal{R}(g^*)) \\ \mathbb{E}\|\hat{\alpha}_c\|_2^2 &\preceq \frac{\log^2 n \log \mathcal{N}_{2n}}{n} + \log^2 n (\mathcal{R}(g_{\mathcal{G}}^*) - \mathcal{R}(g^*)), \end{aligned}$$

where \mathbb{E} is taken with respect to $(\mathbf{X}_i, Y_i)_{i=1}^n$.

Now, we further explore how the error relies on the FNN structure and the function class to which g^* belongs. We consider the Hölder class, which is broad enough to cover most applications. In particular, denote $\lceil a \rceil$ and $\lfloor a \rfloor$ to be the smallest integer no less than a and the largest integer strictly smaller than a , respectively. Let \mathbb{N}^+ be the set of positive integers and \mathbb{N}_0 be the set of nonnegative integers. Let $\beta = s + r$, $r \in (0, 1]$ and $s = \lfloor \beta \rfloor \in \mathbb{N}_0$. For a finite constant $B_0 > 0$, the Hölder class $\mathcal{H}_{\beta}([0, 1]^d, B_0)$ is defined as

$$\begin{aligned} \mathcal{H}_{\beta}([0, 1]^d, B_0) = \{g : [0, 1]^d \mapsto \mathbb{R}, \max_{\|\alpha\|_1 \leq s} \|\partial^{\alpha} g\|_{\infty} \leq B_0, \\ \max_{\|\alpha\|_1 = s} \sup_{x \neq y} \frac{|\partial^{\alpha} g(x) - \partial^{\alpha} g(y)|}{\|x - y\|_2^r} \leq B_0\}, \end{aligned}$$

where $\partial^{\alpha} = \partial^{\alpha_1} \dots \partial^{\alpha_d}$ with $\alpha = (\alpha_1, \dots, \alpha_d)^{\top} \in \mathbb{N}_0^d$ and $\|\alpha\|_1 = \sum_{i=1}^d |\alpha_i|$.

Based on Theorem 3.3 of [Jiao et al. \(2023\)](#) for the approximation error in terms of FNN structures and Theorem 3 and 7 of [Bartlett et al. \(2019\)](#) for the bounding covering number, we can conclude the following Corollary 3.1 from Theorem 3.1:

Corollary 3.1 *Given Hölder smooth functions $g^* \in \mathcal{H}_\beta([0, 1]^d, B_0)$, for any $D \in \mathbb{N}^+$, $W \in \mathbb{N}^+$, under conditions of Theorem 3.1, conditions of Theorem 3.3 in [Jiao et al. \(2023\)](#) and Theorem 3 and 7 in [Bartlett et al. \(2019\)](#), if the FNN with a ReLU activation function has width $\mathcal{W} = c(\lfloor \beta \rfloor + 1)^2 d^{\lfloor \beta \rfloor + 1} W \lceil \log_2(8W) \rceil$ and depth $\mathcal{D} = c(\lfloor \beta \rfloor + 1)^2 D \lceil \log_2(8D) \rceil$ and $\lambda_1 \preceq n^{-1} \mathcal{S} \mathcal{D} \log(\mathcal{S})/d + (WD)^{-4\beta/d}/d$ and $\lambda_2 \preceq n^{-1} \mathcal{S} \log(\mathcal{S})/\mathcal{W}^2 + (WD)^{-4\beta/d}/(\mathcal{W}^2 \mathcal{D})$, then*

$$\begin{aligned}\mathbb{E}[d((\hat{\alpha}, \hat{\theta}), \Theta)] &\preceq (\log^2 n) n^{-1} \mathcal{S} \mathcal{D} \log(\mathcal{S}) + (WD)^{-4\beta/d} (\log^2 n). \\ \mathbb{E}\|\hat{\alpha}_c\|_2^2 &\preceq (\log^2 n) n^{-1} \mathcal{S} \mathcal{D} \log(\mathcal{S}) + (WD)^{-4\beta/d} (\log^2 n).\end{aligned}$$

To facilitate reading, Theorem 3.3 of [Jiao et al. \(2023\)](#) and Theorems 3 and 7 of [Bartlett et al. \(2019\)](#) are also shown in Lemmas and in Appendix. In Corollary 3.1, the first term comes from the covering number of \mathcal{G} , which is bounded by its VC dimension $\log \mathcal{N}_{2n}(n^{-1}, \|\cdot\|_\infty, \mathcal{G}|_x) = O(\mathcal{S} \mathcal{D} \log(\mathcal{S}/n^{-1}))$ ([Bartlett et al. 2019](#)), where \mathcal{S} and \mathcal{D} are the total number of parameters and hidden layers, respectively. The second term follows from the approximation results from [Jiao et al. \(2023\)](#) that $\|g^* - g_{\mathcal{G}}^*\|_\infty \leq 18B_0(\lfloor \beta \rfloor + 1)^2 d^{\lfloor \beta \rfloor + \max\{\beta, 1\}/2} (WD)^{-2\beta/d}$ and $\mathbb{E}(\mathcal{R}(g_{\mathcal{G}}^*) - \mathcal{R}(g^*)) \simeq \mathbb{E}|g_{\mathcal{G}}^* - g^*|^2$, where $A \simeq B$ represents $A \preceq B$ and $B \preceq A$.

Corollary 3.2 *Suppose the conditions of Corollary 3.1 hold. If $\lambda_1 \preceq n^{-1} \mathcal{S} \mathcal{D} \log(\mathcal{S})/d + (WD)^{-4\beta/d}/d$ and $\lambda_2 \preceq n^{-1} \mathcal{S} \log(\mathcal{S})/\mathcal{W}^2 + (WD)^{-4\beta/d}/(\mathcal{W}^2 \mathcal{D})$, for any $j = 1, \dots, d$ and $k = d + 1, \dots, p$, it holds that*

$$\Pr(\{|\hat{\alpha}_j| \geq \tau_d\} \cap \{|\hat{\alpha}_k| \leq \tau_d\}) \rightarrow 1,$$

where τ_d is defined in Condition (C1).

4 Computation

Optimising the composite objective

$$\mathcal{J}(g, \boldsymbol{\alpha}) = \frac{1}{n} \sum_{i=1}^n \left\{ Y_i - g(\boldsymbol{\alpha} \odot \mathbf{X}_i) \right\}^2 + \lambda_1 \|\boldsymbol{\alpha}\|_1 + \lambda_2 \sum_{l=1}^{\mathcal{D}} (\|\mathbf{W}_l - \mathbf{I}\|_1 + |c_l|) \quad (11)$$

is challenging because the L_1 penalties on $\boldsymbol{\alpha}$ and on each $\mathbf{W}_l - \mathbf{I}$ are nondifferentiable at zero, yet we need exact zeros to identify both irrelevant inputs and redundant layers. We therefore employ a periodic hard-thresholding (truncation). Continuous shrinkage via these gradient descent steps ensures that small coefficients approach zero, while exact zeros are enforced by truncation every K iterations.

In the truncation step, any α_j satisfying $|\alpha_j| \leq \tau_1$ is set to zero, and any layer l for which $\|\mathbf{W}_l - \mathbf{I}\|_1 \leq \tau_2$ is collapsed by resetting $\mathbf{W}_l = \mathbf{I}$. Threshold τ_1 is selected based on validation performance, and we follow [Scardapane et al. \(2017\)](#) in fixing $\tau_2 = 10^{-2}$ for synthetic studies and 10^{-3} for real data. By combining subgradient shrinkage with periodic truncation, the algorithm achieves stable convergence, exact sparsity in both $\boldsymbol{\alpha}$ and network depth, and full compatibility with GPU-accelerated training pipelines.

Algorithm 2: Truncation procedure

Input : gate vector $\boldsymbol{\alpha}$; weight matrices $\{\mathbf{W}_l\}$; thresholds τ_1, τ_2

Output: $\boldsymbol{\alpha}_{\text{trunc}}, \{\mathbf{W}_l^{\text{trunc}}\}$

```
1  $\boldsymbol{\alpha}_{\text{trunc}} \leftarrow \boldsymbol{\alpha}$ 
2 for  $j = 1$  to  $d$  do
3   if  $|\alpha_j| \leq \tau_1$  then
4      $\alpha_j \leftarrow 0$ 
5 for  $l = 1$  to  $D$  do
6   if  $\|\mathbf{W}_l - \mathbf{I}\|_1 \leq \tau_2$  then
7      $\mathbf{W}_l \leftarrow \mathbf{I}$ 
8 return  $\boldsymbol{\alpha}_{\text{trunc}}, \{\mathbf{W}_l^{\text{trunc}}\}$ 
```

5 Simulations

We conduct simulation studies to evaluate the empirical performance of the proposed neural network-based variable selection method. In particular, we assess its ability to identify the true set of active predictors and compare it against several widely used approaches: Bayesian Kernel Machine Regression (BKMR), SHapley Additive exPlanations (SHAP), and DeepLIFT. The evaluation focuses on variable selection accuracy under a complex nonlinear model with sparse signal.

5.1 Consistency of Variable Selection

Data are generated from the nonlinear model

$$Y = X_0^3 (X_2^2 + X_5) - |X_7| \cos(X_8) + \varepsilon,$$

where $\varepsilon \sim N(0, 1)$ and each predictor $X_j \sim N(0, 1)$ independently for $j = 0, \dots, 199$. Only five coordinates $\{0, 2, 5, 7, 8\}$ enter the truth, while the remaining $d - 5 = 195$ variables

are noise. We take $n = 1000$ samples and repeat the entire simulation 100 times to assess variability.

We compare our method against five established approaches. Bayesian kernel machine regression (BKMR) (Bobb et al. 2015) fits a Gaussian-process-type model and uses posterior inclusion probabilities for variable selection. SHapley additive explanations (SHAP) (Lundberg & Lee 2017) compute Shapley values post hoc on a pretrained neural network to rank feature importance. DeepLIFT (Shrikumar et al. 2017) is a backpropagation-based attribution method that compares activations to a reference and assigns contribution scores to each input. GLNN (Scardapane et al. 2017) applies group Lasso regularization to neural networks, penalizing groups of weights. Deep feature selection (DPS) (Li et al. 2016, Chen et al. 2021) incorporates sparsity constraints via selection layers embedded in deep architectures. For SHAP and DeepLIFT, we use the same network architecture as our method but without additional adaptive thresholding or depth adjustment, while for GLNN and DPS, we use the architectures specified in their original papers. For all competing methods except BKMR and the proposed method, the top five features are selected by weight magnitude.

Selection accuracy is quantified by the following metrics:

$$\text{Precision} = \frac{|\hat{S}_n \cap S^*|}{|\hat{S}_n|}, \quad \text{Recall} = \frac{|\hat{S}_n \cap S^*|}{|S^*|}, \quad F_1 = \frac{2 \text{Precision} \times \text{Recall}}{\text{Precision} + \text{Recall}}.$$

Table 1 reports the mean and standard deviation of these metrics over 100 simulation replicates.

Table 1: Variable selection performance across competing methods.

Method	Precision	Recall	F1 Score
Proposed	0.927 (0.150)	0.880 (0.183)	0.879 (0.135)
BKMR	0.025 (0.000)	1.000 (0.000)	0.049 (0.000)
SHAP	0.780 (0.060)	0.780 (0.060)	0.780 (0.060)
DeepLIFT	0.720 (0.133)	0.720 (0.133)	0.720 (0.133)
GLNN	0.460 (0.100)	0.460 (0.100)	0.460 (0.100)
DPS	0.244 (0.083)	0.244 (0.083)	0.244 (0.083)

As shown in Table 1, our proposed method achieves an F_1 score of approximately 0.88, significantly outperforming competing approaches. BKMR, despite achieving perfect recall, exhibits extremely low precision and consequently poor overall selection performance ($F_1 \approx 0.05$), indicating severe over-selection. SHAP and DeepLIFT yield moderate selection accuracy but lag behind our proposed method, likely due to their post hoc attribution nature that ignores structured sparsity during training. GLNN and DPS show considerably weaker performance, reflecting limitations in selecting highly relevant nonlinear features under limited depth or overly restrictive sparsity constraints. These findings underscore the advantage of embedding adaptive sparsity constraints and automatic depth selection directly into the neural network training process, thereby substantially enhancing variable selection accuracy and interpretability in high-dimensional, nonlinear modeling scenarios.

5.2 Post-selection Inference

After demonstrating the consistency of our variable selection procedure, we examine its impact on post-selection inference. To this end, we test the null hypothesis

$$H_0 : E(Y | X_1, Z) = E(Y | Z),$$

where Z denotes the set of covariates conditioned upon. In the “no-selection” scenario, Z comprises all predictors except X_1 ; in the post-selection scenario, Z includes only those features retained by our variable-selection procedure (excluding X_1). We then apply the permutation-based test outlined in Section 2.3 to the inference data D_2 under both scenarios, and report the empirical Type I error rates in Table 2.

Table 2: Empirical Type I error rates for testing the null hypothesis $H_0 : E(Y | X_1, Z) = E(Y | Z)$ with sample size $n = 1000$ and 500 simulation replicates. Results are shown for inference conducted with and without a preceding variable selection step.

Inference setting	Type I error
No selection	0.13
Post-selection	0.01

Table 2 demonstrates that inference without prior selection inflates the Type I error to 13%, whereas conditioning on the data-driven subset restores nominal control at 1%. This confirms that our post-selection inference procedure maintains valid error rates even after feature selection.

6 Real Data Application

The real data analysis uses the Early Life Exposure to Environmental Toxicants (ELEMENT) Project. ELEMENT consists of three mother–child cohorts recruited in Mexico City from 1994 to 2005. More than 2,000 women and their children were enrolled and followed from pregnancy through adolescence. We apply these data to evaluate a nonparametric Neural Network Machine Regression (NNMR) method with statistical inference. Our main goal is to identify which prenatal exposures are most strongly associated with infant

growth. Infant growth is measured by WHO anthropometric z-scores considering age and sex. Measurements are collected at regular visits from birth to age five, as well as during cholesterol substudies and at the P20 follow up. The analysis includes a high dimensional panel of dietary patterns grouped by food categories for both mothers and children. We exclude records with missing or implausible z-scores and standardize all exposure variables before modeling.

We evaluated the performance of our Neural Network Machine Regression (NNMR) method for variable selection in high dimensional dietary data, using infant growth z-scores as the outcome. We compared NNMR to the competing method mentioned in section 5. All methods were applied to a dataset containing child and mother dietary exposures, with performance evaluated by Akaike Information Criterion (AIC) calculated on separate training and test datasets.

Table 3: Average AIC and computation time (seconds) for six competing methods applied to the ELEMENT dietary exposure data. Reported values are means with standard deviations in parentheses, calculated on test sets across 100 replicates.

Method	AIC	Time (s)
NNMR	2164.98 (23.66)	6.74 (1.20)
BKMR	2230.27 (23.71)	78.21 (20.31)
SHAP	2166.99 (25.33)	87.01 (8.86)
DeepLIFT	2162.45 (23.33)	3.66 (0.56)
GroupLASSO	2195.56 (41.16)	2.68 (0.43)
DFS	2167.62 (23.36)	7.69 (1.59)

Table 3 shows that NNMR achieves competitive AIC values and computation times compared with DeepLIFT, while outperforming SHAP, DFS, and Group LASSO, and substantially

improving upon BKMR. The poorer performance of BKMR reflects its tendency to select excessively large models, often including nearly all variables. DeepLIFT and SHAP yield prediction errors comparable to NNMR, since they share the same underlying model, but DeepLIFT tends to select the smallest variable set. Group LASSO exhibits unstable behavior, either selecting nearly all variables or only one or two. By contrast, NNMR demonstrates modest variability in AIC across splits, highlighting its stable generalization ability.

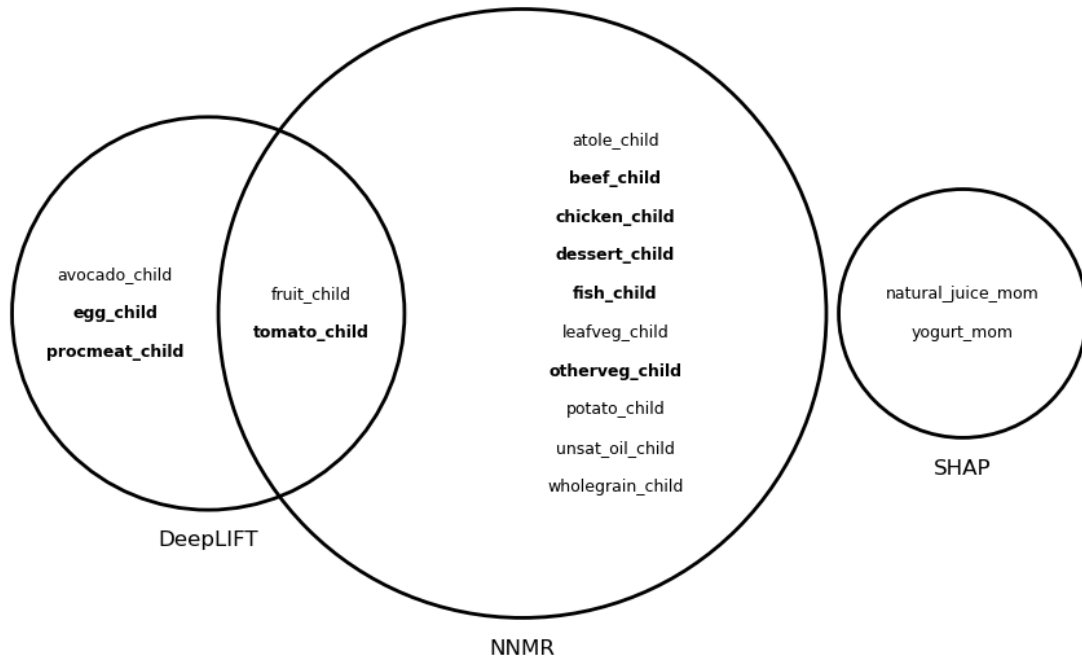


Figure 2: Venn diagram of dietary exposures selected by NNMR, SHAP, and DeepLIFT in the ELEMENT study. Displayed are variables with selection frequency exceeding 20% across 100 replicates. Variables in bold indicate those that remained statistically significant after applying the post-selection inference procedure.

Figure 2 summarizes variable selection via a Venn diagram, comparing NNMR, SHAP, and DeepLIFT. To improve interpretability, we display only variables selected with frequency exceeding 20% across 100 replicates. The complete results are provided in the Supplementary

Materials. Consistent with prior observations, BKMR selects nearly all exposures, while Group LASSO exhibits unstable behavior. DFS selects only `milk_child`, while SHAP emphasizes maternal food groups. In contrast, NNMR and DeepLIFT consistently highlight child dietary exposures with higher and more coherent selection frequencies.

We then applied the inference procedure in Section 2.3 to the union of variables identified by NNMR, DFS, DeepLIFT, and SHAP, using an inference split not employed for selection. Variables highlighted in red in Figure 2 were found to be statistically significant predictors of growth z-scores, the majority of which were prioritized by NNMR.

The five variables uniquely retained by NNMR after inference align closely with established findings in the nutritional epidemiology literature. Higher intake of beef, zinc, and choline during infancy has been linked to improved inhibitory control and attention at ages 3 to 5 years (Wilk et al. 2022). Chicken production and consumption in nutrition sensitive agricultural programs have been shown to benefit child growth in low income settings (Passarelli et al. 2020). Fish serves as a nutrient-dense protein source, rich in vitamins, minerals, and essential fatty acids (Yilmaz et al. 2018). Frequent dessert consumption is associated with increased risk of overweight, a major determinant of growth z-scores (Barroso et al. 2016). Finally, the `otherveg` category, which includes zucchini, cucumber, and green beans, reflects the importance of dietary diversity for child development (Arimond & Ruel 2004, Thorne-Lyman et al. 2019). Collectively, these results underscore the biological plausibility of the predictors identified by NNMR and their relevance to early life growth.

7 Discussion

We have introduced Neural Network Machine Regression (NNMR), an integrated neural network framework designed for simultaneous feature selection, nonlinear function estimation, and rigorous post-selection inference in high-dimensional data analysis. By embedding a

trainable gating layer coupled with an L_1 regularization strategy and an adaptive thresholding mechanism, NNMR achieves direct sparsity enforcement in input features and hidden network layers, resulting in highly compact and interpretable models.

Our theoretical analysis provides guarantees for consistent recovery of the relevant feature set, supported by a minimax-optimal upper bound on the risk under mild assumptions. Additionally, our integrated split-sample permutation testing approach ensures robust control over type I error rates, mitigating false-positive risks commonly encountered in high-dimensional inference.

Empirical results from extensive simulations illustrate that NNMR outperforms established approaches such as BKMR, SHAP, DeepLIFT, GLNN, and DPS in terms of variable selection precision, recall, and overall accuracy (F_1 score). While BKMR achieves high recall at the cost of severe over-selection, and SHAP and DeepLIFT offer moderate accuracy, NNMR clearly demonstrates superior performance in identifying true predictors and controlling selection errors. GLNN and DPS exhibit considerably lower accuracy, underscoring the limitations of traditional sparsity approaches in capturing complex nonlinear relationships.

Real-data applications further validate NNMR’s practical utility by demonstrating its capability to pinpoint meaningful, interpretable predictors in complex biomedical datasets. Unlike post hoc attribution methods, which are often unstable under feature collinearity, NNMR’s built-in sparsity ensures accurate identification of genuinely inactive features. The dynamic pruning of unnecessary layers also facilitates resource-efficient implementations suitable for GPU acceleration.

In summary, NNMR bridges interpretability and predictive modeling power by embedding statistically rigorous variable selection, adaptive model optimization, and valid inference within a unified training framework. This integrative approach positions NNMR as a robust and versatile solution for modern high-dimensional statistical and deep learning applications.

References

Anthony, M., Bartlett, P. L., Bartlett, P. L. et al. (1999), *Neural network learning: Theoretical foundations*, Vol. 9, cambridge university press Cambridge.

Arimond, M. & Ruel, M. T. (2004), 'Dietary diversity is associated with child nutritional status: evidence from 11 demographic and health surveys', *The Journal of nutrition* **134**(10), 2579–2585.

Barroso, C. S., Roncancio, A., Moramarco, M. W., Hinojosa, M. B., Davila, Y. R., Mendias, E. & Reifsnyder, E. (2016), 'Food security, maternal feeding practices and child weight-for-length', *Applied Nursing Research* **29**, 31–36.

Bartlett, P. L., Harvey, N., Liaw, C. & Mehrabian, A. (2019), 'Nearly-tight vc-dimension and pseudodimension bounds for piecewise linear neural networks', *The Journal of Machine Learning Research* **20**(1), 2285–2301.

Bobb, J. F., Valeri, L., Claus Henn, B., Christiani, D. C., Wright, R. O., Mazumdar, M., Godleski, J. J. & Coull, B. A. (2015), 'Bayesian kernel machine regression for estimating the health effects of multi-pollutant mixtures', *Biostatistics* **16**(3), 493–508.

Cai, Z., Lei, J. & Roeder, K. (2022), 'Model-free prediction test with application to genomics data', *Proceedings of the National Academy of Sciences* **119**(34), e2205518119.

Chen, Y., Gao, Q., Liang, F. & Wang, X. (2021), 'Nonlinear variable selection via deep neural networks', *Journal of Computational and Graphical Statistics* **30**(2), 484–492.

Cox, D. R. (1975), 'A note on data-splitting for the evaluation of significance levels', *Biometrika* pp. 441–444.

Fan, J. & Li, R. (2001), 'Variable selection via nonconcave penalized likelihood and its oracle properties', *Journal of the American statistical Association* **96**(456), 1348–1360.

Fan, J. & Lv, J. (2008), 'Sure independence screening for ultrahigh dimensional feature space',

Journal of the Royal Statistical Society Series B: Statistical Methodology **70**(5), 849–911.

Hastie, T. J. (2017), 'Generalized additive models', *Statistical models in S* pp. 249–307.

Hurvich, C. M. & Tsai, C. (1990), 'The impact of model selection on inference in linear regression', *The American Statistician* **44**(3), 214–217.

Jiao, Y., Shen, G., Lin, Y. & Huang, J. (2023), 'Deep nonparametric regression on approximate manifolds: Nonasymptotic error bounds with polynomial prefactors', *The Annals of Statistics* **51**(2), 691–716.

Lei, J. (2020), 'Cross-validation with confidence', *Journal of the American Statistical Association* **115**(532), 1978–1997.

Li, Y., Chen, C.-Y. & Wasserman, W. W. (2016), 'Deep feature selection: theory and application to identify enhancers and promoters', *Journal of Computational Biology* **23**(5), 322–336.

Lundberg, S. M. & Lee, S.-I. (2017), 'A unified approach to interpreting model predictions', *Advances in neural information processing systems* **30**.

Passarelli, S., Ambikapathi, R., Gunaratna, N. S., Madzorera, I., Canavan, C. R., Noor, A. R., Worku, A., Berhane, Y., Abdelmenan, S., Sibanda, S. et al. (2020), 'A chicken production intervention and additional nutrition behavior change component increased child growth in ethiopia: a cluster-randomized trial', *The Journal of Nutrition* **150**(10), 2806–2817.

Scardapane, S., Comminiello, D., Hussain, A. & Uncini, A. (2017), 'Group sparse regularization for deep neural networks', *Neurocomputing* **241**, 81–89.

Shrikumar, A., Greenside, P. & Kundaje, A. (2017), Learning important features through

propagating activation differences, *in* ‘International conference on machine learning’, PMLR, pp. 3145–3153.

Sundararajan, M., Taly, A. & Yan, Q. (2017), Axiomatic attribution for deep networks, *in* ‘International conference on machine learning’, PMLR, pp. 3319–3328.

Tan, Z., Zhou, L. & Lin, H. (2024), ‘Generative adversarial learning with optimal input dimension and its adaptive generator architecture’, *arXiv preprint arXiv:2405.03723*.

Thorne-Lyman, A. L., Shrestha, M., Fawzi, W. W., Pasqualino, M., Strand, T. A., Kvestad, I., Hysing, M., Joshi, N., Lohani, M. & Miller, L. C. (2019), ‘Dietary diversity and child development in the far west of nepal: a cohort study’, *Nutrients* **11**(8), 1799.

Tibshirani, R. (1996), ‘Regression shrinkage and selection via the lasso’, *Journal of the Royal Statistical Society Series B: Statistical Methodology* **58**(1), 267–288.

Wilk, V. C., McGuire, M. K. & Roe, A. J. (2022), ‘Early life beef consumption patterns are related to cognitive outcomes at 1–5 years of age: An exploratory study’, *Nutrients* **14**(21), 4497.

Yılmaz, E., Aydin, M., Yıldırım, A. & Şahin, P. (2018), ‘The importance of consumption of fish meat in early childhood period in terms of healthy development’, *Süleyman Demirel Üniversitesi Eğirdir Su Ürünleri Fakültesi Dergisi* **14**(4), 357–364.

Appendix

Full List of Variable Selection Results in ELEMENT Study

Table 4 presents the complete list of variables along with their selection frequencies across repeated data splits for the proposed Neural Network Machine Regression (NNMR), SHAP, DeepLIFT, and DFS methods. For SHAP, only variables with selection frequencies greater

than 0.05 are displayed to improve readability. Since BKMR and GroupLASSO consistently selected nearly all variables with frequencies close to 1.0 and 0.45, their results are omitted from the table for brevity. This presentation highlights the variables that were most consistently identified as important by the methods that demonstrated more selective behavior.

Table 4: Variables with nonzero selection frequencies across repeated splits for NNMR, SHAP (only ≥ 0.05 shown), DeepLIFT, and DFS. BKMR and GroupLASSO selected nearly all variables (frequencies ≈ 1.0 and 0.45) and are omitted for brevity.

feature	NNMR	SHAP	DeepLIFT	DFS
<i>atole_child</i>	0.38	–	–	–
<i>avocado_child</i>	0.15	–	0.25	–
<i>beef_child</i>	0.41	–	0.19	–
<i>chicken_child</i>	0.43	–	0.15	–
<i>chili_child</i>	0.09	–	–	–
<i>chips_child</i>	0.02	–	–	–
<i>corn_tortilla_child</i>	0.01	0.08	–	–
<i>corncob_child</i>	0.13	–	–	–
<i>corncob_mom</i>	–	0.06	–	–
<i>cruveg_child</i>	0.01	–	–	–
<i>dessert_child</i>	0.31	0.06	–	–
<i>egg_child</i>	0.16	–	0.30	–
<i>fish_child</i>	0.23	–	0.03	–
<i>fish_mom</i>	–	0.06	–	–

Continued on next page

feature	NNMR	SHAP	DeepLIFT	DFS
<i>fruit_child</i>	0.38	—	0.74	—
<i>fruit_mom</i>	—	0.07	—	—
<i>hf_dairy_child</i>	0.01	—	0.16	—
<i>jam_child</i>	0.01	—	—	—
<i>leafveg_child</i>	0.39	—	—	—
<i>legumes_child</i>	0.03	—	—	—
<i>milk_child</i>	0.02	—	0.19	1.00
<i>natural_juice_mom</i>	—	0.48	—	—
<i>organmeat_child</i>	0.16	—	0.03	—
<i>otherveg_child</i>	0.35	—	—	—
<i>pork_child</i>	0.04	—	0.09	—
<i>potato_child</i>	0.29	—	0.04	—
<i>procmeat_child</i>	0.02	0.06	0.23	—
<i>refgrain_child</i>	0.13	0.12	—	—
<i>refgrain_mom</i>	—	0.08	—	—
<i>soup_child</i>	0.18	—	—	—
<i>sugar_beverages_child</i>	0.05	0.07	—	—
<i>sugar_beverages_mom</i>	—	0.13	—	—
<i>tomato_child</i>	0.39	—	0.22	—
<i>unsat_oil_child</i>	0.43	—	—	—
<i>wholegrain_child</i>	0.26	—	—	—
<i>yeveg_child</i>	0.02	0.09	—	—

Continued on next page

feature	NNMR	SHAP	DeepLIFT	DFS
<i>yogurt_child</i>	0.01	—	0.15	—
<i>yogurt_mom</i>	—	0.32	—	—

Proofs of Theorems

Denote $\mathcal{R}_n(g_{\alpha, \theta}) = \frac{1}{n} \sum_{i=1}^n (Y_i - g(\mathbf{X}_i))^2$, for $g \in \mathcal{G}(\alpha, \theta)$. For any independent and identically distributed (i.i.d.) samples $D_n = \{\mathbf{X}_i, Y_i\}_{i=1}^n$ with sample size n . Define

$$S(g_{\alpha, \theta}, \mathbf{X}_i) = (Y_i - g(\mathbf{X}_i))^2 - (Y_i - g^*(\mathbf{X}_i))^2.$$

Let $D'_n = \{\mathbf{X}'_i, Y'_i\}$ be another sample independent of D_n , and write

$$L(g_{\alpha, \theta}, \mathbf{X}'_i) = \mathbb{E}_{D'_n} (S(g_{\alpha, \theta}, \mathbf{X}'_i)) - 2S(g_{\alpha, \theta}, \mathbf{X}_i).$$

Recall that $g_{\theta}(\alpha \odot \cdot) \in \mathcal{G}(\alpha, \theta)$ and

$$(\hat{\alpha}, \hat{\theta}) \in \arg \min \mathcal{L}_n(g_{\alpha, \theta}) = \arg \min_{(\alpha, \theta)} \left[\mathcal{R}_n(g_{\alpha, \theta}) + \lambda_1 \|\alpha\|_1 + \lambda_2 \sum_{l=1}^{\mathcal{D}} \|\mathbf{W}_l - \mathbf{I}\|_1 \right].$$

Covering number. Given a δ -uniform covering of \mathcal{G} , we denote the centers of the balls by $g_q, q = 1, \dots, \mathcal{N}_{2n}$, where $\mathcal{N}_{2n} = \sup_{\mathbf{x}} \mathcal{N}_{2n}(\delta, \|\cdot\|_{\infty}, \mathcal{G}|_{\mathbf{x}})$ is the uniform covering number with radius δ under the norm $\|\cdot\|_{\infty}$. By the definition of covering, there exists a q^* such that $\|g_{\hat{\alpha}, \hat{\theta}} - g_{q^*}\|_{\infty} \leq \delta$ on $\mathbf{x} \in (\mathbf{X}_1, \dots, \mathbf{X}_n, \mathbf{X}'_1, \dots, \mathbf{X}'_n)$. Let $A \preceq B$ represent $A \leq cB$ for a positive constant c .

Proof of Theorem 3.1. Let $(\check{\alpha}, \check{\theta}) \in \Theta$ such that

$$(\check{\alpha}, \check{\theta}) \in \arg \min_{(\alpha, \theta) \in \Theta} \mathbb{E} \left[d \left((\hat{\alpha}, \hat{\theta}), \Theta \right) \right].$$

Without loss of generality, we slightly abuse notation by writing $\sum_{l=1}^{\mathcal{D}} \|\mathbf{W}_l - \mathbf{I}\|_1$ to denote $\sum_{l=1}^{\mathcal{D}} (\|\mathbf{W}_l - \mathbf{I}\|_1 + |c_l|)$, where the intercept term is absorbed into the weight matrix \mathbf{W}_l of the neural network. Then, it follows that

$$\mathcal{R}_n(g_{\hat{\alpha}, \hat{\theta}}) + \lambda_1 \|\hat{\alpha}\|_1 + \lambda_2 \sum_{l=1}^{\mathcal{D}} \|\hat{\mathbf{W}}_l - \mathbf{I}\|_1 \leq \mathcal{R}_n(g_{\check{\alpha}, \check{\theta}}) + \lambda_1 \|\check{\alpha}\|_1 + \lambda_2 \sum_{l=1}^{\mathcal{D}} \|\check{\mathbf{W}}_l - \mathbf{I}\|_1.$$

For the expected excess risk, we have the following decomposition,

$$\begin{aligned} & \mathbb{E} \left(\mathcal{R}(g_{\hat{\alpha}, \hat{\theta}}) - \mathcal{R}(g_{\check{\alpha}, \check{\theta}}) \right) \\ = & \mathbb{E} \left(\mathcal{R}(g_{\hat{\alpha}, \hat{\theta}}) - \mathcal{R}_n(g_{\hat{\alpha}, \hat{\theta}}) \right) + \mathbb{E} \left(\mathcal{R}_n(g_{\hat{\alpha}, \hat{\theta}}) - \mathcal{R}_n(g_{\check{\alpha}, \check{\theta}}) \right) \end{aligned} \quad (3)$$

$$\begin{aligned} & + \mathbb{E} \left(\mathcal{R}_n(g_{\check{\alpha}, \check{\theta}}) - \mathcal{R}(g_{\check{\alpha}, \check{\theta}}) \right) \\ \leq & I_1 + \mathbb{E}_{D_n} \left[\lambda_1 (\|\check{\alpha}\|_1 - \|\hat{\alpha}\|_1) + \lambda_2 \sum_{l=1}^{\mathcal{D}} \left(\|\check{\mathbf{W}}_l - \mathbf{I}\|_1 - \|\hat{\mathbf{W}}_l - \mathbf{I}\|_1 \right) \right]. \end{aligned} \quad (4)$$

Note that the first term has the following upper bound:

$$\begin{aligned} I_1 &:= \mathbb{E} \left(\mathcal{R}(g_{\hat{\alpha}, \hat{\theta}}) - \mathcal{R}_n(g_{\hat{\alpha}, \hat{\theta}}) \right) \\ &= \mathbb{E}_{D_n} \left\{ n^{-1} \sum_{i=1}^n \left[\mathbb{E}_{D'_n} \left(n^{-1} \sum_{i=1}^n (Y'_i - g_{\hat{\theta}}(\hat{\alpha} \odot \mathbf{X}'_i))^2 \right) \right. \right. \\ &\quad \left. \left. - (Y_i - g_{\hat{\theta}}(\hat{\alpha} \odot \mathbf{X}_i))^2 \right] \right\} \\ &= \mathbb{E}_{D_n} \left\{ n^{-1} \sum_{i=1}^n \left[\mathbb{E}_{D'_n} \left(n^{-1} \sum_{i=1}^n S(g_{\hat{\alpha}, \hat{\theta}}, \mathbf{X}'_i) \right) - 2S(g_{\hat{\alpha}, \hat{\theta}}, \mathbf{X}'_i) \right] \right\} \\ &\quad + \mathbb{E}_{D_n} \left\{ n^{-1} \sum_{i=1}^n \left[(Y_i - g_{\hat{\theta}}(\hat{\alpha} \odot \mathbf{X}_i))^2 - (Y_i - g_{\check{\theta}}(\check{\alpha} \odot \mathbf{X}_i))^2 \right] \right\} \\ &\quad + \mathbb{E}_{D_n} \left\{ n^{-1} \sum_{i=1}^n S(g_{\check{\theta}, \check{\alpha}}, \mathbf{X}'_i) \right\} \\ &\leq I_{11} + \mathbb{E}_{D_n} \left[\lambda_1 (\|\check{\alpha}\|_1 - \|\hat{\alpha}\|_1) + \lambda_2 \sum_{l=1}^{\mathcal{D}} \left(\|\check{\mathbf{W}}_l - \mathbf{I}\|_1 - \|\hat{\mathbf{W}}_l - \mathbf{I}\|_1 \right) \right] \\ &\quad + (\mathcal{R}(g_{\check{\alpha}, \check{\theta}}) - \mathcal{R}(g^*)). \end{aligned} \quad (6)$$

Next, we will give an upper bound of I_{11} and handle it with truncation and classical chaining

technique of empirical processes. According to the definition of $S(g_{\alpha, \theta}, \mathbf{X}_i)$, we have

$$\begin{aligned}
& \left| S(g_{\hat{\alpha}, \hat{\theta}}, \mathbf{X}'_i) - S(g_{q^*}, \mathbf{X}'_i) \right| \\
&= \left| 2Y_i(g_{\hat{\theta}}(\hat{\alpha} \odot \mathbf{X}_i) - g_{q^*}(\mathbf{X}_i)) + (g_{\hat{\theta}}^2(\hat{\alpha} \odot \mathbf{X}_i) - g_{q^*}^2(\mathbf{X}_i)) \right| \\
&\leq (2|Y_i| + 2\mathcal{B})\delta,
\end{aligned}$$

and

$$\begin{aligned}
& \left| L(g_{\hat{\alpha}, \hat{\theta}}, \mathbf{X}'_i) - L(g_{q^*}, \mathbf{X}'_i) \right| \\
&\leq \mathbb{E}_{D'_n} \left(\left| S(g_{\hat{\alpha}, \hat{\theta}}, \mathbf{X}'_i) - S(g_{q^*}, \mathbf{X}'_i) \right| \right) + 2 \left| S(g_{\hat{\alpha}, \hat{\theta}}, \mathbf{X}'_i) - S(g_{q^*}, \mathbf{X}'_i) \right| \\
&\leq 3(\mathbb{E}|Y_i| + \mathcal{B} + |Y_i|)\delta.
\end{aligned}$$

Then, it follows that

$$\mathbb{E}_{D_n} \left(n^{-1} \sum_{i=1}^n \left| L(g_{\hat{\alpha}, \hat{\theta}}, \mathbf{X}'_i) - L(g_{q^*}, \mathbf{X}'_i) \right| \right) \leq 6(\mathbb{E}|Y_i| + \mathcal{B})\delta,$$

which leads to

$$\mathbb{E}_{D_n} \left(n^{-1} \sum_{i=1}^n L(g_{\hat{\alpha}, \hat{\theta}}, \mathbf{X}'_i) \right) \leq \mathbb{E}_{D_n} \left(n^{-1} \sum_{i=1}^n L(g_{q^*}, \mathbf{X}'_i) \right) + 6(\mathbb{E}|Y_i| + \mathcal{B})\delta. \quad (7)$$

Let $0 < \beta_n$ be a positive number who may depend on the sample size n . Denote $T_{\beta_n}Y = Y$ if $Y \leq \beta_n$ and $T_{\beta_n}Y = \beta_n$ otherwise. Define the function $g_{\beta_n}^*$ by

$$g_{\beta_n}^*(\mathbf{x}) = \arg \min_{g: \|g\|_\infty < \mathcal{B}} \mathbb{E} \left[(T_{\beta_n}Y_i - g(\mathbf{X}_i))^2 \mid \mathbf{X}_i = \mathbf{x} \right].$$

For any $g \in \mathcal{G}(\alpha, \theta)$, let $S_{\beta_n}(g_{\alpha, \theta}, \mathbf{X}'_i) = (T_{\beta_n}Y_i - g_{\theta}(\alpha \odot \mathbf{X}_i))^2 - (T_{\beta_n}Y_i - g_{\beta_n}^*(\mathbf{X}_i))^2$. Then,

we have

$$\begin{aligned}
\mathbb{E}(S(g_{\alpha,\theta}, \mathbf{X}'_i)) &= \mathbb{E}(S_{\beta_n}(g_{\alpha,\theta}, \mathbf{X}'_i)) + \mathbb{E}\left[\left(Y_i - g_{\theta}(\boldsymbol{\alpha} \odot \mathbf{X}_i)\right)^2 - \left(T_{\beta_n}Y_i - g_{\theta}(\boldsymbol{\alpha} \odot \mathbf{X}_i)\right)^2\right] \\
&\quad - \mathbb{E}\left[\left(Y_i - g^*(\mathbf{X}_i)\right)^2 - \left(T_{\beta_n}Y_i - g^*(\mathbf{X}_i)\right)^2\right] \\
&\quad - \mathbb{E}\left[\left(T_{\beta_n}Y_i - g^*(\mathbf{X}_i)\right)^2 - \left(T_{\beta_n}Y_i - g_{\beta_n}^*(\mathbf{X}_i)\right)^2\right] \\
&\leq \mathbb{E}(S_{\beta_n}(g_{\alpha,\theta}, \mathbf{X}'_i)) + \mathbb{E}\left(Y_i^2 - (T_{\beta_n}Y_i)^2 - 2(Y_i - T_{\beta_n}Y_i)g_{\theta}(\boldsymbol{\alpha} \odot \mathbf{X}_i)\right) \\
&\quad - \mathbb{E}\left(Y_i^2 - (T_{\beta_n}Y_i)^2 - 2(Y_i - T_{\beta_n}Y_i)g^*(\mathbf{X}_i)\right) \\
&\leq \mathbb{E}(S_{\beta_n}(g_{\alpha,\theta}, \mathbf{X}'_i)) + 4\mathbb{E}(|Y_i|I(Y_i > \beta_n))\mathcal{B},
\end{aligned}$$

and

$$\begin{aligned}
\mathbb{E}(S_{\beta_n}(g_{\alpha,\theta}, \mathbf{X}'_i)) &= \mathbb{E}(S(g_{\alpha,\theta}, \mathbf{X}'_i)) - \mathbb{E}\left[\left(Y_i - g_{\theta}(\boldsymbol{\alpha} \odot \mathbf{X}_i)\right)^2 - \left(T_{\beta_n}Y_i - g_{\theta}(\boldsymbol{\alpha} \odot \mathbf{X}_i)\right)^2\right] \\
&\quad - \mathbb{E}\left[\left(T_{\beta_n}Y_i - g_{\beta_n}^*(\mathbf{X}_i)\right)^2 - \left(Y_i - g_{\beta_n}^*(\mathbf{X}_i)\right)^2\right] \\
&\quad - \mathbb{E}\left[\left(Y_i - g_{\beta_n}^*(\mathbf{X}_i)\right)^2 - \left(Y_i - g^*(\mathbf{X}_i)\right)^2\right] \\
&\leq \mathbb{E}(S(g_{\alpha,\theta}, \mathbf{X}'_i)) - \mathbb{E}\left(Y_i^2 - (T_{\beta_n}Y_i)^2 - 2(Y_i - T_{\beta_n}Y_i)g_{\theta}(\boldsymbol{\alpha} \odot \mathbf{X}_i)\right) \\
&\quad + \mathbb{E}\left(Y_i^2 - (T_{\beta_n}Y_i)^2 - 2(Y_i - T_{\beta_n}Y_i)g_{\beta_n}^*(\mathbf{X}_i)\right) \\
&\leq \mathbb{E}(S(g_{\alpha,\theta}, \mathbf{X}'_i)) + 4\mathbb{E}(|Y_i|I(Y_i > \beta_n))\mathcal{B},
\end{aligned}$$

which leads to

$$\left| \mathbb{E}(S(g_{\alpha,\theta}, \mathbf{X}'_i) - S_{\beta_n}(g_{\alpha,\theta}, \mathbf{X}'_i)) \right| \leq 4\mathbb{E}(|Y_i|I(Y_i > \beta_n))\mathcal{B}.$$

Then,

$$\begin{aligned}
&\left| \mathbb{E}_{D_n}\left[\frac{1}{n} \sum_{i=1}^n \left(L(g_{q^*}, \mathbf{X}'_i) - L_{\beta_n}(g_{q^*}, \mathbf{X}'_i)\right)\right] \right| \\
&\leq \left| \mathbb{E}_{D'_n}(S(g_{q^*}, \mathbf{X}'_i) - S_{\beta_n}(g_{q^*}, \mathbf{X}'_i)) \right| + 2\left| \mathbb{E}_{D_n}(S(g_{q^*}, \mathbf{X}'_i) - S_{\beta_n}(g_{q^*}, \mathbf{X}'_i)) \right| \\
&\leq 12\mathbb{E}(|Y_i|I(Y_i > \beta_n))\mathcal{B}.
\end{aligned} \tag{8}$$

On the other hand, for any $g \in \mathcal{G}(\boldsymbol{\alpha}, \boldsymbol{\theta})$, we have

$$|S_{\beta_n}(g, \mathbf{X}'_i)| \leq 5(\beta_n + \mathcal{B})^2,$$

$$\sigma_S^2(g) := \text{Var}(S_{\beta_n}(g, \mathbf{X}'_i)) \leq \mathbb{E}\{S_{\beta_n}^2(g, \mathbf{X}'_i)\} \leq 5(\beta_n + \mathcal{B})^2 \mathbb{E}(S_{\beta_n}(g, \mathbf{X}'_i)).$$

Following the Bernstein inequality, for any $t > 0$, let $u = t/2 + \sigma_S^2(g)/(10(\beta_n + \mathcal{B})^2)$, we have

$$\begin{aligned} & P \left\{ n^{-1} \sum_{i=1}^n L_{\beta_n}(g_q, \mathbf{X}'_i) > t \right\} \\ = & P \left\{ \mathbb{E}_{D'_n}(S_{\beta_n}(g_q, \mathbf{X}'_i)) - n^{-1} 2 \sum_{i=1}^n S_{\beta_n}(g_q, \mathbf{X}'_i) > t \right\} \\ = & P \left\{ \mathbb{E}_{D'_n}\{S_{\beta_n}(g_q, \mathbf{X}'_i)\} - \frac{1}{n} \sum_{i=1}^n S_{\beta_n}(g_q, \mathbf{X}'_i) > \frac{t}{2} + \frac{1}{2} \mathbb{E}_{D'_n}\{S_{\beta_n}(g_q, \mathbf{X}'_i)\} \right\} \\ \leq & P \left\{ \mathbb{E}_{D'_n}\{S_{\beta_n}(g_q, \mathbf{X}'_i)\} - \frac{1}{n} \sum_{i=1}^n S_{\beta_n}(g_q, \mathbf{X}'_i) > \frac{t}{2} + \frac{1}{2} \frac{\sigma_S^2(g)}{5(\beta_n + \mathcal{B})^2} \right\} \\ \leq & \exp\left(-\frac{nu^2}{2\sigma_S^2(g) + 20u(\beta_n + \mathcal{B})^2/3}\right) \\ \leq & \exp\left(-\frac{nu^2}{20u(\beta_n + \mathcal{B})^2 + 20u(\beta_n + \mathcal{B})^2/3}\right) \\ \leq & \exp\left(-\frac{1}{20 + 20/3} \frac{nu}{(\beta_n + \mathcal{B})^2}\right) \\ \leq & \exp\left(-\frac{1}{40 + 40/3} \frac{nt}{(\beta_n + \mathcal{B})^2}\right) \\ = & \exp\left(-\frac{Cn t}{(\beta_n + \mathcal{B})^2}\right). \end{aligned}$$

This leads to a tail probability bound of $n^{-1} \sum_{i=1}^n L_{\beta_n}(g_{q^*}, \mathbf{X}'_i)$, that is,

$$P \left\{ n^{-1} \sum_{i=1}^n L_{\beta_n}(g_{q^*}, \mathbf{X}'_i) > t \right\} \leq 2\mathcal{N}_{2n} \exp\left(-\frac{Cn t}{(\beta_n + \mathcal{B})^2}\right).$$

Then for $a_n > 0$,

$$\begin{aligned} \mathbb{E}_{D_n} \left[\frac{1}{n} \sum_{i=1}^n L_{\beta_n}(g_{q^*}, \mathbf{X}'_i) \right] & \leq a_n + \int_{a_n}^{\infty} P \left\{ \frac{1}{n} \sum_{i=1}^n L_{\beta_n}(g_{q^*}, \mathbf{X}'_i) > t \right\} dt \\ & \leq a_n + \int_{a_n}^{\infty} 2\mathcal{N}_{2n} \exp\left(-\frac{Cn t}{(\beta_n + \mathcal{B})^2}\right) dt \\ & \leq a_n + 2\mathcal{N}_{2n} \exp\left(-a_n \frac{Cn}{(\beta_n + \mathcal{B})^2}\right) \frac{(\beta_n + \mathcal{B})^2}{Cn}. \end{aligned}$$

Choosing $a_n = \log 2\mathcal{N}_{2n} \frac{(\beta_n + \mathcal{B})^2}{Cn}$, the above inequality leads to

$$\mathbb{E}_{D_n} \left[\frac{1}{n} \sum_{i=1}^n L_{\beta_n}(g_{q^*}, \mathbf{X}'_i) \right] \leq \frac{C(\beta_n + \mathcal{B})^2 (\log 2\mathcal{N}_{2n} + 1)}{n}. \quad (9)$$

Combining inequalities (7), (8), and (9), we have

$$\begin{aligned}
I_{11} &= \mathbb{E}_{D_n} \left(n^{-1} \sum_{i=1}^n L(g_{\hat{\alpha}, \hat{\theta}}, \mathbf{X}'_i) \right) \\
&\leq \mathbb{E}_{D_n} \left(n^{-1} \sum_{i=1}^n L(g_{q^*}, \mathbf{X}'_i) \right) + 6 (\mathbb{E}|Y_i| + \mathcal{B}) \delta \\
&\leq \mathbb{E}_{D_n} \left(n^{-1} \sum_{i=1}^n L_{\beta_n}(g_{q^*}, \mathbf{X}'_i) \right) + 6 (\mathbb{E}|Y_i| + \mathcal{B}) \delta + 12\mathbb{E}(|Y_i|I(Y_i > \beta_n))\mathcal{B} \\
&\leq \frac{C(\beta_n + \mathcal{B})^2(\log 2\mathcal{N}_{2n} + 1)}{n} + 6 (\mathbb{E}|Y_i| + \mathcal{B}) \delta + 12\mathbb{E}(|Y_i|I(Y_i > \beta_n))\mathcal{B}.
\end{aligned}$$

Let $\beta_n = \log n$ and $\delta = n^{-1}$. Under conditions (C2) and (C3), using the above inequalities, we obtain that

$$I_{11} \preceq \frac{C \log^2 n \log \mathcal{N}_{2n}}{n}. \quad (10)$$

Then, combining inequalities (3), (5), and (10), using the condition that $\mathbb{E} \left[d \left((\boldsymbol{\alpha}, \boldsymbol{\theta}), \boldsymbol{\Theta} \right) \right] \leq c\mathbb{E} \left(\mathcal{R}(g_{\boldsymbol{\alpha}, \boldsymbol{\theta}}) - \mathcal{R}(g_{\check{\boldsymbol{\alpha}}, \check{\boldsymbol{\theta}}}) \right)$, we can obtain

$$\begin{aligned}
\mathbb{E} \left[d \left((\hat{\boldsymbol{\alpha}}, \hat{\boldsymbol{\theta}}), \boldsymbol{\Theta} \right) \right] &= \mathbb{E} \left(\left\| (\hat{\boldsymbol{\alpha}}, \hat{\boldsymbol{\theta}}) - (\check{\boldsymbol{\alpha}}, \check{\boldsymbol{\theta}}) \right\|_2^2 \right) \leq c \mathbb{E} \left\{ \mathcal{R}(g_{\hat{\boldsymbol{\alpha}}, \hat{\boldsymbol{\theta}}}) - \mathcal{R}(g_{\check{\boldsymbol{\alpha}}, \check{\boldsymbol{\theta}}}) \right\} \\
&\leq c I_1 + c \mathbb{E} \left[\lambda_1 \left(\|\check{\boldsymbol{\alpha}}\|_1 - \|\hat{\boldsymbol{\alpha}}\|_1 \right) + \lambda_2 \sum_{l=1}^{\mathcal{D}} \left(\|\check{\mathbf{W}}_l - \mathbf{I}\|_1 - \|\hat{\mathbf{W}}_l - \mathbf{I}\|_1 \right) \right] \\
&\leq c I_{11} + c \lambda_1 \mathbb{E} [\|\check{\boldsymbol{\alpha}} - \hat{\boldsymbol{\alpha}}\|_1] + c \lambda_2 \sum_{l=1}^{\mathcal{D}} \mathbb{E} [\|\check{\mathbf{W}}_l - \hat{\mathbf{W}}_l\|_1] \\
&\leq c \frac{C \log^2 n \log \mathcal{N}_{2n} (n^{-1}, \|\cdot\|_\infty, \mathcal{G} | \mathbf{x})}{n} + c \lambda_1 \sqrt{d} \mathbb{E} [\|\check{\boldsymbol{\alpha}} - \hat{\boldsymbol{\alpha}}\|_2] \\
&\quad + c \lambda_2 \sum_{l=1}^{\mathcal{D}} \mathcal{W} \mathbb{E} [\|\check{\mathbf{W}}_l - \hat{\mathbf{W}}_l\|_F],
\end{aligned} \quad (11)$$

To let the right side of the above inequality to be minimum, we have that

$$\begin{aligned}
\lambda_1^2 &\leq \frac{c \log^2 n \log \mathcal{N}_{2n}}{nd} + \frac{c(\mathcal{R}(g_{\check{\boldsymbol{\alpha}}, \check{\boldsymbol{\theta}}}) - \mathcal{R}(g^*))}{d}, \\
\lambda_2^2 &\leq \frac{c \log^2 n \log \mathcal{N}_{2n}}{n \mathcal{W}^2 \mathcal{D}} + \frac{c(\mathcal{R}(g_{\check{\boldsymbol{\alpha}}, \check{\boldsymbol{\theta}}}) - \mathcal{R}(g^*))}{\mathcal{W}^2 \mathcal{D}},
\end{aligned} \quad (12)$$

Note that using Young's inequality, we have

$$\begin{aligned}\mathbb{E}\left[c\lambda_1\sqrt{d}\|\check{\boldsymbol{\alpha}}-\hat{\boldsymbol{\alpha}}\|_2\right] &\leq \frac{1}{2}\mathbb{E}\left[\|\check{\boldsymbol{\alpha}}-\hat{\boldsymbol{\alpha}}\|_2^2\right] + \frac{c^2\lambda_1^2d}{2}. \\ \mathbb{E}\left[c\lambda_2\mathcal{W}\|\check{\mathbf{W}}_l-\hat{\mathbf{W}}_l\|_F\right] &\leq \frac{1}{2}\mathbb{E}\left[\|\check{\mathbf{W}}_l-\hat{\mathbf{W}}_l\|_F^2\right] + \frac{c^2\lambda_2^2\mathcal{W}^2}{2}.\end{aligned}\tag{13}$$

Combining inequalities (11), (12) and (13), we can obtain that

$$\begin{aligned}\mathbb{E}\left[d\left((\hat{\boldsymbol{\alpha}}, \hat{\boldsymbol{\theta}}), \Theta\right)\right] &\leq c\left\{\frac{\log^2 n \log \mathcal{N}_{2n}}{n} + \left(\mathcal{R}(g_{\check{\boldsymbol{\alpha}}, \check{\boldsymbol{\theta}}}) - \mathcal{R}(g^*)\right) + \lambda_1^2 d + \lambda_2^2 \mathcal{W}^2 \mathcal{D}\right\}. \\ &\leq c\left\{\frac{\log^2 n \log \mathcal{N}_{2n}}{n} + \left(\mathcal{R}(g_{\check{\boldsymbol{\alpha}}, \check{\boldsymbol{\theta}}}) - \mathcal{R}(g^*)\right)\right\}.\end{aligned}$$

Let $(\boldsymbol{\alpha}_s^*, \boldsymbol{\theta}_s^*) \in \arg \min_{\boldsymbol{\alpha}_s, \boldsymbol{\theta}_s} \mathcal{R}(g_{\boldsymbol{\alpha}_s, \boldsymbol{\theta}_s}) = \arg \min_{\boldsymbol{\alpha}_s, \boldsymbol{\theta}_s} \mathbb{E}(Y - g_{\boldsymbol{\theta}_s}(\boldsymbol{\alpha}_s \odot \mathbf{X}_s))^2$. Define $\Theta_s = \{(\boldsymbol{\alpha}_s, \boldsymbol{\theta}_s) : \mathcal{R}(g_{\boldsymbol{\alpha}_s, \boldsymbol{\theta}_s}) = \mathcal{R}(g_{\boldsymbol{\alpha}_s^*, \boldsymbol{\theta}_s^*})\}$. Define $d((\boldsymbol{\alpha}_s, \boldsymbol{\theta}_s), \Theta_s) = \min_{(\boldsymbol{\alpha}_s, \boldsymbol{\theta}_s) \in \Theta_s} \|(\hat{\boldsymbol{\alpha}}_s, \hat{\boldsymbol{\theta}}_s) - (\boldsymbol{\alpha}_s, \boldsymbol{\theta}_s)\|_2^2$, and write $(\check{\boldsymbol{\alpha}}_s, \check{\boldsymbol{\theta}}_s) \in \arg \min_{(\boldsymbol{\alpha}_s, \boldsymbol{\theta}_s) \in \Theta_s} \|(\hat{\boldsymbol{\alpha}}_s, \hat{\boldsymbol{\theta}}_s) - (\boldsymbol{\alpha}_s, \boldsymbol{\theta}_s)\|_2^2$, where $\check{\boldsymbol{\theta}}_s = \{(\check{W}_{s,l}, \check{c}_{s,l}), l = 0, \dots, L\}$. Denote $\tilde{\boldsymbol{\theta}} \in \arg \min_{\boldsymbol{\theta}} \mathcal{R}(g_{\check{\boldsymbol{\alpha}}, \boldsymbol{\theta}})$, where $\tilde{\boldsymbol{\alpha}} = (\check{\boldsymbol{\alpha}}_s, \mathbf{0})$. Then, it follows from Lemma 7.1 that $(\check{\boldsymbol{\alpha}}_s, \mathbf{0}, \tilde{\boldsymbol{\theta}}) \in \Theta$.

It follows from

$$\mathcal{R}_n(g_{\hat{\boldsymbol{\alpha}}, \hat{\boldsymbol{\theta}}}) + \lambda_1 \|\hat{\boldsymbol{\alpha}}\|_1 + \lambda_2 \sum_{l=1}^{\mathcal{D}} \|\hat{\mathbf{W}}_l - \mathbf{I}\|_1 \leq \mathcal{R}_n(g_{\check{\boldsymbol{\alpha}}_s, \mathbf{0}, \check{\boldsymbol{\theta}}}) + \lambda_1 \|\check{\boldsymbol{\alpha}}_s\|_1 + \lambda_2 \sum_{l=1}^{\mathcal{D}} \|\check{\mathbf{W}}_l - \mathbf{I}\|_1,$$

that

$$\begin{aligned}\lambda_1 \|\hat{\boldsymbol{\alpha}}_c\|_1 &\leq \mathcal{R}_n(g_{\check{\boldsymbol{\alpha}}_s, \mathbf{0}, \check{\boldsymbol{\theta}}}) - \mathcal{R}_n(g_{\hat{\boldsymbol{\alpha}}, \hat{\boldsymbol{\theta}}}) + \lambda_1 (\|\check{\boldsymbol{\alpha}}_s\|_1 - \|\hat{\boldsymbol{\alpha}}_s\|_1) + \lambda_2 \sum_{l=1}^{\mathcal{D}} (\|\check{\mathbf{W}}_l - \mathbf{I}\|_1 - \|\hat{\mathbf{W}}_l - \mathbf{I}\|_1).\end{aligned}\tag{14}$$

Insert and subtract population risks gives:

$$\begin{aligned}\lambda_1 \|\hat{\boldsymbol{\alpha}}_c\|_1 &\leq \left[\mathcal{R}(g_{\check{\boldsymbol{\alpha}}_s, \mathbf{0}, \check{\boldsymbol{\theta}}}) - \mathcal{R}(g_{\hat{\boldsymbol{\alpha}}, \hat{\boldsymbol{\theta}}})\right] + \left[\mathcal{R}(g_{\hat{\boldsymbol{\alpha}}, \hat{\boldsymbol{\theta}}}) - \mathcal{R}_n(g_{\hat{\boldsymbol{\alpha}}, \hat{\boldsymbol{\theta}}})\right] \\ &\quad + \lambda_1 (\|\check{\boldsymbol{\alpha}}_s\|_1 - \|\hat{\boldsymbol{\alpha}}_s\|_1) + \lambda_2 \sum_{l=1}^{\mathcal{D}} (\|\check{\mathbf{W}}_l - \mathbf{I}\|_1 - \|\hat{\mathbf{W}}_l - \mathbf{I}\|_1).\end{aligned}\tag{15}$$

Because $(\check{\boldsymbol{\alpha}}_s, \mathbf{0}, \check{\boldsymbol{\theta}}) \in \Theta$ we have $\mathcal{R}(g_{\check{\boldsymbol{\alpha}}_s, \mathbf{0}, \check{\boldsymbol{\theta}}}) = \mathcal{R}(g^*) \leq \mathcal{R}(g_{\hat{\boldsymbol{\alpha}}, \hat{\boldsymbol{\theta}}})$, hence the first bracket in (15) is nonpositive and can be dropped:

$$\begin{aligned} \lambda_1 \|\hat{\boldsymbol{\alpha}}_c\|_1 &\leq \left[\mathcal{R}(g_{\hat{\boldsymbol{\alpha}}, \hat{\boldsymbol{\theta}}}) - \mathcal{R}_n(g_{\hat{\boldsymbol{\alpha}}, \hat{\boldsymbol{\theta}}}) \right] + \lambda_1 \left(\|\check{\boldsymbol{\alpha}}_s\|_1 - \|\hat{\boldsymbol{\alpha}}_s\|_1 \right) \\ &\quad + \lambda_2 \sum_{l=1}^{\mathcal{D}} \left(\|\check{\mathbf{W}}_l - \mathbf{I}\|_1 - \|\hat{\mathbf{W}}_l - \mathbf{I}\|_1 \right). \end{aligned} \quad (16)$$

For the gate term, $\|\check{\boldsymbol{\alpha}}_s\|_1 - \|\hat{\boldsymbol{\alpha}}_s\|_1 \leq \|\check{\boldsymbol{\alpha}}_s - \hat{\boldsymbol{\alpha}}_s\|_1 \leq \sqrt{d} \|\check{\boldsymbol{\alpha}}_s - \hat{\boldsymbol{\alpha}}_s\|_2$. For the depth term, by triangle inequality and ℓ_1 - ℓ_2 ,

$$\sum_{l=1}^{\mathcal{D}} \left\| \check{\mathbf{W}}_l - \mathbf{I} \right\|_1 - \left\| \hat{\mathbf{W}}_l - \mathbf{I} \right\|_1 \leq \sum_{l=1}^{\mathcal{D}} \left\| \check{\mathbf{W}}_l - \hat{\mathbf{W}}_l \right\|_1 \leq \sqrt{S} \|\check{\boldsymbol{\theta}} - \hat{\boldsymbol{\theta}}\|_2,$$

where $S = \mathcal{W}^2 \mathcal{D}$ is the total number of scalar parameters in θ . Therefore (16) yields

$$\lambda_1 \|\hat{\boldsymbol{\alpha}}_c\|_1 \leq \left[\mathcal{R}(g_{\hat{\boldsymbol{\alpha}}, \hat{\boldsymbol{\theta}}}) - \mathcal{R}_n(g_{\hat{\boldsymbol{\alpha}}, \hat{\boldsymbol{\theta}}}) \right] + \lambda_1 \sqrt{d} \|\check{\boldsymbol{\alpha}}_s - \hat{\boldsymbol{\alpha}}_s\|_2 + \lambda_2 \sqrt{S} \|\check{\boldsymbol{\theta}} - \hat{\boldsymbol{\theta}}\|_2. \quad (17)$$

With Young's inequality, we have:

$$\lambda_1 \|\hat{\boldsymbol{\alpha}}_c\|_1 \leq \left[\mathcal{R}(g_{\hat{\boldsymbol{\alpha}}, \hat{\boldsymbol{\theta}}}) - \mathcal{R}_n(g_{\hat{\boldsymbol{\alpha}}, \hat{\boldsymbol{\theta}}}) \right] + \frac{1}{2} \|\check{\boldsymbol{\alpha}}_s - \hat{\boldsymbol{\alpha}}_s\|_2^2 + \frac{1}{2} \lambda_1^2 d + \frac{1}{2} \|\check{\boldsymbol{\theta}} - \hat{\boldsymbol{\theta}}\|_2^2 + \frac{1}{2} \lambda_2^2 S. \quad (18)$$

Taking expectations:

$$\mathbb{E}[\lambda_1 \|\hat{\boldsymbol{\alpha}}_c\|_1] \leq \mathbb{E} \left[\mathcal{R}(g_{\hat{\boldsymbol{\alpha}}, \hat{\boldsymbol{\theta}}}) - \mathcal{R}_n(g_{\hat{\boldsymbol{\alpha}}, \hat{\boldsymbol{\theta}}}) \right] + \frac{1}{2} \mathbb{E} \left[\|(\hat{\boldsymbol{\alpha}}_s, \hat{\boldsymbol{\theta}}) - (\check{\boldsymbol{\alpha}}_s, \check{\boldsymbol{\theta}})\|_2^2 \right] + \frac{1}{2} \lambda_1^2 d + \frac{1}{2} \lambda_2^2 S. \quad (19)$$

which leads to

$$\mathbb{E}(\|\hat{\boldsymbol{\alpha}}_c\|_2^2) \leq \mathbb{E}(\|\hat{\boldsymbol{\alpha}}_c\|_1^2) \leq \frac{c \log^2 n \log \mathcal{N}_{2n}}{n} + c \left(\mathcal{R}(g_{\check{\boldsymbol{\alpha}}_s, \mathbf{0}, \check{\boldsymbol{\theta}}}) - \mathcal{R}(g^*) \right).$$

Lemmas

Lemma 7.1 *Under condition (C1), if $p = O(\log^c n)$ for some positive constant c , for $(\boldsymbol{\alpha}^*, \boldsymbol{\theta}^*) \in \arg \min_{g \in \mathcal{G}(\boldsymbol{\alpha}, \boldsymbol{\theta})} \mathbb{E}(Y_i - g(\mathbf{X}_i))^2$, then it follows that*

(i) $|\alpha_j^*| \geq \tau_d$, for $\forall j = 1, \dots, d$ and some positive constant c ;

(ii) there exists a solution $(\boldsymbol{\alpha}^*, \boldsymbol{\theta}^*)$, such that $\boldsymbol{\alpha}_c^* = 0$.

Proof of Lemma 7.1.

(i) Suppose that there exists a $(\boldsymbol{\alpha}^*, \boldsymbol{\theta}^*)$ such that $|\alpha_j^*| < c\tau_d$ for at least one $j \in \{1, \dots, d\}$. Then, for any random vector $\mathbf{X} \in [0, 1]^p$, we construct the vector $\mathbf{X}_{[j]}(0) = (X_{[1]}, \dots, X_{[j-1]}, 0, X_{[j+1]}, \dots, X_{[p]})$, clearly, $|g_{\boldsymbol{\theta}^*}(\boldsymbol{\alpha}^* \odot \mathbf{X}_{[j]}(0)) - g_{\boldsymbol{\theta}^*}(\boldsymbol{\alpha}^* \odot \mathbf{X})| \leq c\tau_d$ for some positive constant c . Based on the definition that $g_{\mathcal{G}}^* = \arg \min_{g \in \mathcal{G}(\boldsymbol{\alpha}, \boldsymbol{\theta})} \mathbb{E}(Y_i - g(\boldsymbol{\alpha} \odot \mathbf{X}_i))^2$, that

$$g_{\boldsymbol{\theta}^*}(\boldsymbol{\alpha}^* \odot \mathbf{X}_{[j]}(0)) = \mathbb{E}(Y \mid \mathbf{X}_{[-j]} = \mathbf{x}_{[-j]}), \text{ and } g_{\boldsymbol{\theta}^*}(\boldsymbol{\alpha}^* \odot \mathbf{X}) = \mathbb{E}(Y \mid \mathbf{X} = \mathbf{x}).$$

It contradicts condition (C2). Thus, for any $j = 1, \dots, d$, $|\alpha_j^*| \geq \tau_d$ for some positive constant c .

(ii) Let $(\boldsymbol{\alpha}_s^*, \boldsymbol{\theta}_s^*) \in \arg \min_{\boldsymbol{\alpha}_s, \boldsymbol{\theta}_s} \mathcal{R}(g_{\boldsymbol{\alpha}_s, \boldsymbol{\theta}_s}) = \arg \min_{\boldsymbol{\alpha}_s, \boldsymbol{\theta}_s} \mathbb{E}(Y - g_{\boldsymbol{\theta}_s}(\boldsymbol{\alpha}_s \odot \mathbf{X}_s))^2$. Define $\boldsymbol{\Theta}_s = \{(\boldsymbol{\alpha}_s, \boldsymbol{\theta}_s) : \mathcal{R}(g_{\boldsymbol{\alpha}_s, \boldsymbol{\theta}_s}) = \mathcal{R}(g_{\boldsymbol{\alpha}_s^*, \boldsymbol{\theta}_s^*})\}$. Define $d((\boldsymbol{\alpha}_s, \boldsymbol{\theta}_s), \boldsymbol{\Theta}_s) = \min_{(\boldsymbol{\alpha}_s, \boldsymbol{\theta}_s) \in \boldsymbol{\Theta}_s} \|(\hat{\boldsymbol{\alpha}}_s, \hat{\boldsymbol{\theta}}_s) - (\boldsymbol{\alpha}_s, \boldsymbol{\theta}_s)\|_2^2$, and write $(\check{\boldsymbol{\alpha}}_s, \check{\boldsymbol{\theta}}_s) \in \arg \min_{(\boldsymbol{\alpha}_s, \boldsymbol{\theta}_s) \in \boldsymbol{\Theta}_s} \|(\hat{\boldsymbol{\alpha}}_s, \hat{\boldsymbol{\theta}}_s) - (\boldsymbol{\alpha}_s, \boldsymbol{\theta}_s)\|_2^2$, where $\check{\boldsymbol{\theta}}_s = \{(\check{A}_{s,l}, \check{c}_{s,l}), l = 0, \dots, L\}$. Denote $\tilde{\boldsymbol{\theta}} \in \arg \min_{\boldsymbol{\theta}} \mathcal{R}(g_{\tilde{\boldsymbol{\alpha}}, \boldsymbol{\theta}})$, where $\tilde{\boldsymbol{\alpha}} = (\check{\boldsymbol{\alpha}}_s, \mathbf{0})$. Let $\check{\boldsymbol{\theta}} = \{(\tilde{A}_l, \tilde{c}_l), l = 0, \dots, L\}$ with $\tilde{c}_l = \check{c}_{s,l}$ for $l = 0, \dots, L$, $\tilde{A}_l = \check{A}_{s,l}$ for $l = 1, \dots, L$, and $\tilde{A}_0 = (\check{A}_{s,0}, A_{c,0})$. Then, based on the definition (2), it is easy to show that

$$\mathcal{R}(g_{\tilde{\boldsymbol{\alpha}}, \tilde{\boldsymbol{\theta}}}) \leq \mathcal{R}(g_{\check{\boldsymbol{\alpha}}_s, \check{\boldsymbol{\theta}}_s}) = \mathcal{R}(g_{\check{\boldsymbol{\alpha}}_s, \check{\boldsymbol{\theta}}_s}) = \mathcal{R}(g_{\boldsymbol{\alpha}^*, \boldsymbol{\theta}^*}).$$

Clearly, $(\tilde{\boldsymbol{\alpha}}, \tilde{\boldsymbol{\theta}})$ is the solution.

Lemma 7.2 (Approximation error, (Theorem 3.3 in [Jiao et al. 2023](#)))

Given Hölder smooth functions $g^* \in \mathcal{H}_\beta([0, 1]^d, B_0)$, for any $D \in \mathbb{N}^+$ and $W \in \mathbb{N}^+$, there exists a function $g_{\mathcal{G}}^*$ implemented by a ReLU feedforward neural network with width $\mathcal{W} = 38(\lfloor \beta \rfloor + 1)^2 d^{\lfloor \beta \rfloor + 1} W \lceil \log_2(8W) \rceil$ and depth $\mathcal{D} = 21(\lfloor \beta \rfloor + 1)^2 D \lceil \log_2(8D) \rceil$ such that

$$|g^* - g_{\mathcal{G}}^*| \leq 18B_0(\lfloor \beta \rfloor + 1)^2 d^{\lfloor \beta \rfloor + \max\{\beta, 1\}/2} (WD)^{-2\beta/d},$$

for all $x \in [0, 1]^d \setminus \Omega([0, 1]^d, K, \delta)$ where

$$\Omega([0, 1]^d, K, \delta) = \bigcup_{i=1}^d \{x = [x_1, \dots, x_d]^T : x_i \in \bigcup_{k=1}^{K-1} (k/K - \delta, k/K)\},$$

with $K = \lfloor WD \rfloor$ and δ is an arbitrary number in $(0, 1/(3K)]$.

Lemma 7.3 (*Bounding the covering number, (Theorem 12.2 in [Anthony et al. 1999](#)) and (Theorems 3 and 7 in [Bartlett et al. 2019](#))*)

Let ReLU feedforward neural network \mathcal{G} be a set of real functions from a domain \mathcal{X} to the bounded interval $[0, \mathcal{B}]$. There exists a universal constant C such that the following holds. Given any \mathcal{D}, \mathcal{S} with $\mathcal{S} > C\mathcal{D} > C^2$, there exists network class \mathcal{G} with $\leq \mathcal{D}$ layers and $\leq \mathcal{S}$ parameters with VC-dimension $\geq \mathcal{S}\mathcal{D} \log(\mathcal{S}/\mathcal{D})/C$ and given $\delta > 0$

$$\sup_{\mathbf{x}} \log \mathcal{N}_{2n}(\delta, \|\cdot\|_\infty, \mathcal{G}|_{\mathbf{x}}) = O\left(\mathcal{S}\mathcal{D} \log(\mathcal{S}/\delta)\right).$$